

**Investigating how boundary genes control abscission in *Arabidopsis thaliana***

**By: Laura Corrigan**

**B.Sc. La Cité Collégiale, 2016**

**A thesis submitted to the Faculty of Graduate and Postdoctoral Affairs in partial fulfillment of the requirements for the degree of**

**Master of Science**

**in**

**Biology**

**Carleton University**

**Ottawa, Ontario, Canada**

**© 2018 Laura Corrigan**

## ABSTRACT

The shedding, or abscission, of plant organs occurs in four stages at specialized junctions in the plant called abscission zones (AZs). Premature abscission can pose a problem for farmers by reducing crop yield. Studies in *Arabidopsis thaliana* have identified organ boundary genes *BLADE-ON-PETIOLE1/2* (*BOP1/2*) as essential for the formation of AZs. However, downstream effectors of *BOP1/2* in this process are unknown. To execute developmental programs in inflorescences, *BOP1/2* require TGA basic leucine zipper transcription factors for recruitment to DNA and TALE homeodomain proteins *ATH1* and *KNAT6* for boundary patterning. How these factors contribute to abscission is unclear. Here, I show that TGA and TALE transcription factors contribute to *BOP*-dependent formation of AZs. I also begin to explore a role for this module in organ separation. Collectively, my work reveals a role for boundary genes at different steps of abscission for potential application in crops.

## **ACKNOWLEDGEMENTS**

I would like to express my utmost gratitude to my supervisor, Dr. Shelley Hepworth, for her support, teaching, and patience. She has provided me with much guidance throughout my graduate studies and has been a great female role model in the STEM domain. I am grateful for the opportunities and teaching she has provided me. I would also like to thank Dr. Jenny Bruin and Dr. Thérèse Ouellet for their guidance as my committee advisors and for providing me with suggestions to help me succeed with my research.

My time in the Hepworth lab would not have been enjoyable without my fellow lab members who helped me both academically and emotionally. A special thank you to Adina Popescu and Chris Bergin for teaching me techniques as well as for being good friends. I would also like to thank Ying Wang, Gigi Allam, Omar Al-Juboori, and Kevin Xiong for their cumulative support and guidance through the years.

Furthermore, I would also like to thank my dearest family members Terry, Lucy, and Sara Corrigan, who have all supported me throughout my studies. Finally, I would like to give a special thank you to Kevin Wiles for being my best friend and great support during this stressful and busy time by being an amazing hiking partner, friend and fellow adventure seeker.

Thank you to all.

## PREFACE

This thesis examines the contribution of boundary genes to plant organ abscission. I carried out the majority of work described in this thesis under the supervision of Dr. Shelley Hepworth, Department of Biology, Carleton University and under the co-supervision of Dr. Véronique Pautot, Institute Jean-Pierre Bourgin, France.

Ya Ding carried out the initial characterization of *ath1-3 knat2-5*, *ath1-3 knat6-2*, and *ath1-3 knat2-5 knat6-2* mutant lines to identify abscission defects that formed the starting point of my project. The *ath1-3 knat6-1*, *knat2-5 knat6-1*, and *ath1-3 knat 2-5 knat6-1* plant lines used in my thesis were provided by Véronique Pautot from the Jean-Pierre Bourgin Institute in France. The petal break strength meter was developed by Dr. Jeff Dawson. Michael Jutting assisted with the construction of the load cell and amplifier used by the petal break strength meter. The initial petal break strength measurement experiments were performed by Selena Rorabeck in the early stages of this project. Ying Wang assisted with PCR genotyping and Chris Bergin assisted with the validation of primers for qRT-PCR. Lastly, training and technical assistance of the SEM was provided by Dr. Jianqun Wang.

None of the work described in my thesis has been submitted for publication.

## TABLE OF CONTENTS

ABSTRACT.....	2
ACKNOWLEDGEMENTS.....	3
PREFACE.....	4
TABLE OF CONTENTS.....	5
GENETIC NOMENCLATURE IN <i>ARABIDOPSIS THALIANA</i> .....	7
GLOSSARY OF GENETIC TERMS.....	8
LIST OF ABBREVIATIONS.....	9
LIST OF TABLES.....	11
LIST OF FIGURES.....	12
CHAPTER 1 : INTRODUCTION.....	14
1.1 Thesis overview.....	14
1.2 Abscission.....	15
1.2.1 Roles of abscission in nature.....	15
1.2.2 Abscission in crops.....	15
1.3 Model plant species for abscission.....	16
1.4 Step 1 – AZ initiation.....	18
1.4.1 <i>BLADE-ON-PETIOLE</i> genes.....	18
1.4.2 <i>TGA bZIP</i> genes.....	19
1.4.3 <i>TALE homeobox</i> genes.....	20
1.5 Step 2 - AZ cells acquire competency to react to signals.....	21
1.5.1 <i>MADS-box</i> genes.....	21
1.6 Step 3 - activation of abscission.....	22
1.6.1 <i>IDA</i> signaling pathway.....	22
1.6.2 <i>Mechanics of separation</i> .....	24
1.7 Step 4 - differentiation of a protective layer.....	25
1.8 Thesis rationale.....	25
CHAPTER 2 : MATERIALS AND METHODS.....	29
2.1 Plant material and growth conditions.....	29
2.2 Extraction of genomic DNA and genotyping.....	30
2.2 Scanning electron microscopy (SEM).....	30
2.3 Petal break strength.....	31

2.4 Localization of GUS activity.....	33
CHAPTER 3 : RESULTS .....	36
3.1 Progressive loss of ATH1, KNAT6 and KNAT2 activity impairs boundaries in flowers..	36
3.2 Progressive loss of ATH1, KNAT6, and KNAT2 activity impairs floral organ abscission	37
3.3 Clade I TGAs contribute to AZ formation .....	39
3.4 ATH1 functions downstream of BP .....	40
3.5 BOP1/2 contribute to activation of abscission .....	41
CHAPTER 4 : DISCUSSION.....	59
4.1 TALE genes are required for successive steps of abscission .....	59
4.2 Clade I TGAs play a minor role in the sizing of the AZ.....	61
4.3 Interaction with IDA pathway.....	62
4.4 Links between innate immunity and abscission .....	63
4.5 Concluding remarks .....	63
REFERENCES .....	65
SUPPLEMENTARY MATERIALS .....	75

## GENETIC NOMENCLATURE IN *ARABIDOPSIS THALIANA*

Wild type gene: *BOP1*

Wild type protein: BOP1

Loss-of-function mutant (homozygous): *bop1*

Loss-of-function mutant (hemizygous): *bop1/+*

Gain-of-function mutant (dominant): *bop1-6D*

Double mutant: *bop1 bop2*

Promoter fusion to a gene coding region: *35S:BOP1*

Protein fusion: *BOP1-GR*

## **GLOSSARY OF GENETIC TERMS**

Loss-of-function: complete or partial loss of activity

Gain-of-function: ectopic or increased activity

Redundancy: when two or more genes are performing the same function such that inactivation of one of these genes has little or no effect on the phenotype

Homolog: genes sharing a common ancestor in evolution

## LIST OF ABBREVIATIONS

AGL	AGAMOUS-LIKE
ATH	ARABIDOPSIS THALIANA HOMEODOMAIN GENE
AZ	Abscission zone
BAK	BRI1-ASSOCIATED RECEPTOR KINASE
BELL	BEL1-LIKE homeodomain
BOP	BLADE-ON-PETIOLE
BP	BREVIPEDICELLUS
BRI	BRASSINOSTEROID INSENSITIVE
BTB	BROAD COMPLEX, TRAMTRACK, AND BRIC-A-BRAC
Col	Columbia
CST	CAST AWAY
EVR	EVERSHED
FLS	FLAGELLIN-SENSITIVE
FYF	FOREVER YOUNG FLOWER
GUS	$\beta$ -Glucuronidase
HAE	HAESA
HD	Homeodomain
HSL2	HAESA-LIKE
IDA	INFLORESCENCE DEFICIENT IN ABSCISSION
KNAT	KNOTTED-LIKE FROM ARABIDOPSIS THALIANA
KNOX	KNOTTED1-LIKE
MAPK	MITOGEN-ACTIVATED PROTEIN KINASE
NEV	NEVERSHED
POZ	POX VIRUS AND ZINC FINGER
ROS	Reactive oxygen species
SAM	Shoot apical meristem
SEM	Scanning electron microscope/microscopy

SERK	SOMATIC EMBRYOGENESIS RECEPTOR-LIKE KINASE
STM	SHOOT MERISTEMLESS
TALE	THREE-AMINO-ACID-LOOP-EXTENSION
TF	TRANSCRIPTION FACTOR
TGA	TGACG-motif binding
WT	wild type

## **LIST OF TABLES**

<b>Table 2.1: List of genetic materials used in this study</b> .....	34
<b>Table 2.2: List of primers used for genotyping</b> .....	35
<b>Supplemental Table S1. Abscission characteristic descriptions of mutant plants</b> .....	75
<b>Supplemental Table S2. List of qPCR primers</b> .....	76

## LIST OF FIGURES

Figure 1.1 Arabidopsis flower abscission zones and model for abscission. ....	27
Figure 1.2 Schematic representation of thesis hypothesis. ....	28
Figure 3.1 SEM images of wild type and boundary gene mutants. ....	43
Figure 3.2 Abscission analysis of wild type and boundary gene mutants. ....	45
Figure 3.3 Petal break strength measurements for wild type and boundary mutants. ....	46
Figure 3.4 SEM micrographs showing morphology of wild type and boundary mutant receptacles. ....	48
Figure 3.5 Analysis of floral morphology and abscission in <i>tga1 tga4</i> , <i>ath1 tga1</i> , <i>ath1 tga4</i> , and <i>ath1 tga1 tga4</i> mutants. ....	49-50
Figure 3.6 Petal break strength measurements for wild type, <i>tga1 tga4</i> , <i>ath1</i> , <i>ath1 tga1</i> , <i>ath1 tga4</i> , and <i>ath1 tga1 tga4</i> mutants. ....	51
Figure 3.7 SEM micrographs showing morphology of floral AZs in <i>tga1 tga4</i> and <i>ath1</i> , <i>ath1 tga1</i> , <i>ath1 tga4</i> , and <i>ath1 tga1 tga4</i> mutants. ....	52
Figure 3.8 <i>ATH1:GUS</i> expression in wild type and <i>bp-2</i> mutant flowers. ....	53
Figure 3.9 Interaction of <i>BP</i> and <i>ATH1</i> in abscission. ....	55
Figure 3.10 Petal break strength measurements for wild type, <i>bp-2</i> , <i>ath1</i> , and <i>bp-2 ath1</i> mutants. ....	56
Figure 3.11 Abscission phenotype of <i>BOPI</i> overexpressing transgenic plants. ....	58
Supplemental Figure S1. SEM images of wild type and boundary gene mutants. ....	77
Supplemental Figure S2. Inflorescence apices showing the abscission phenotype of 12-week-old wild type and mutant plants. ....	79

<b>Supplemental Figure S3. Measurement of medial and lateral AZ in wild type and mutants.</b> .....	<b>80</b>
<b>Supplemental Figure S4. Abscission analysis of <i>knat2</i>, <i>knat6</i> and <i>knat2 knat6</i> mutants.....</b>	<b>81</b>
<b>Supplemental Figure S5. Morphology of floral AZs in wild type and mutants. ....</b>	<b>82</b>
<b>Supplemental Figure S6. Comparing AZ shape of wild type and <i>bp-2</i> mutant. ....</b>	<b>83</b>
<b>Supplemental Figure S7. Wild-type and mutant siliques stained with Yariv reagent for detection of arabinogalactans in the AZ. ....</b>	<b>84</b>
<b>Supplemental Figure S8. Promoter GUS fusions showing the expression of boundary genes in residuum and secession AZ layers.....</b>	<b>86</b>

## CHAPTER 1 : INTRODUCTION

### 1.1 Thesis overview

The shedding, or abscission, of plant organs such as leaves, flowers, fruits, or seeds is a natural process that allows the distribution of seeds or removal of unwanted organs. Although beneficial in the wild, premature abscission in crops is undesirable because it reduces yield. Abscission takes place at predetermined positions in the plant called abscission zones (AZs). AZs are typically formed at organ boundaries, which represent a layer of cells found at the base of organs where they attach to the plant body. Abscission occurs in four steps: 1) formation of an AZ, 2) AZs gain competence to react to abscission signals, 3) organ separation, and 4) formation of a protective epidermal layer over the scar. Studies in the model plant species, *Arabidopsis thaliana* (Arabidopsis) have identified organ boundary genes *BLADE-ON-PETIOLE1/2* (*BOP1/2*) as essential for the differentiation of AZs. However, downstream effectors of BOP1/2 proteins in this process are unknown. In inflorescences, BOP1/2 interact with TGA (TGACG-motif binding) bZIP (basic leucine zipper) transcription factors for recruitment to DNA and require the downstream activity of three-amino-acid-loop-extension (TALE) homeodomain transcription factors, which are subdivided into KNOX and BELL members that work as heterodimers. BOP1/2-TGA activity depends on at least one BELL factor ARABIDOPSIS THALIANA HOMEODOMAIN GENE1 (ATH1) and one KNOX binding partner KNOTTED-LIKE FROM ARABIDOPSIS THALIANA6 (KNAT6). The role of these factors in the abscission process is only partially characterized. My thesis examines how boundary genes contribute to the abscission process. This work contributes to knowledge of the abscission process, an essential prerequisite for application in crops.

## **1.2 Abscission**

Abscission (from the Latin *ab* = away from and *scindere* = to cleave, meaning “to tear”) is a developmental process that leads to the shedding of organs from the plant body (van Doorn and Stead, 1997). Abscission takes place at dedicated sites in the plant body called abscission zones (AZs). These zones contain cells that are susceptible to signals leading to release of hydrolytic enzymes that precisely degrade the cell wall and pectin-rich middle-lamella that attaches cells together, so that organs can detach (Bleeker and Patterson, 1997; Roberts et al., 2002). This highly coordinated process is worth studying because premature abscission is a major source of crop loss for farmers (Patterson et al., 2016).

### ***1.2.1 Roles of abscission in nature***

Abscission is an essential process in nature. Notably, deciduous plants in the northern hemisphere lose their leaves in the autumn as a means of conserving water and resources for better survival through the winter. Abscission is also crucial for plant reproduction since it releases seeds for growth of the next generation (Patharkar and Walker, 2017). Abscission is also an important “self-pruning” mechanism in plants. When exposed to drought, many plants, such as beans, will shed their leaves. This adaptation allows a plant to conserve energy at a time when nutritional resources are limiting (Pandey et al., 1984; Patharkar and Walker, 2017). Plants also use abscission to discard organs that become damaged by insect feeding or disease. This protective mechanism promotes survival by giving a plant sufficient time and resources to mount an effective immune response (Faeth et al., 1981; Patharkar and Walker, 2017).

### ***1.2.2 Abscission in crops***

In agriculture, abscission is a major limiting factor in crop productivity. Remarkably, early farmers that domesticated crops like wheat (*Triticum monococcum*), rice (*Oryza sativa*), and

legumes selected for natural variants with reduced abscission of seeds (Patterson, 2001). In modern agriculture, knowledge of abscission physiology has led to useful control methods. For example, growers routinely make use of chemical thinning agents to control total fruit load (Celton et al., 2014). Also for example, to prevent apple and citrus trees from dropping their fruits, synthetic auxin and ethylene blockers, which can partially block abscission, are sprayed on trees about a month before harvest (Anthony and Coggins, 1999; Yuan and Carbaugh, 2007; Patharkar and Walker, 2017). The spraying of these agents is beneficial for reducing premature abscission but can have unwanted environmental consequences (Celton et al., 2014). Thus, understanding the molecular mechanism of abscission and producing resistant genotypes is desirable.

The genetic control of abscission is only partly understood. Naturally-occurring mutations that block abscission have been identified in a certain crop species. One famous example is the “jointless” mutant variation of tomato, used in the canning industry due to its lack of pedicel abscission, which causes the calyx and stem to be left behind on the plant when fruit are harvested (Zahara and Scheurerman, 1988; Mao et al., 2000; Patharkar and Walker, 2017). Fruits without the calyx and stem can be safely transported in shipping containers without puncturing other fruits. By better understanding abscission, breeders can develop cultivars that minimize crop loss, leading to better outcomes for farmers.

### **1.3 Model plant species for abscission**

The model plant species *Arabidopsis thaliana* (Arabidopsis) has been instrumental as a discovery tool in plant biology. First documented in the early 1900s by Friedrich Laibach, Arabidopsis was originally selected for genetic research due to its short generation time, small size, and prolific seed production through self-pollination. Arabidopsis quickly gained popularity in the botanical world and continues to be a premier model for plant biology (Koornneef and

Meinke, 2010). Gene mutations in *Arabidopsis* can be easily introduced using chemical mutagens, X-rays, or *Agrobacterium*-mediated approaches. Further, *Arabidopsis* has a small compact diploid genome that is fully sequenced, along with many community resources including cDNA libraries, mutants, transgenic lines, vectors, and transcriptome databases (Somerville and Koornneef, 2002; Koornneef and Meinke, 2010). These and other factors have greatly accelerated the pace of plant biology research worldwide (Somerville and Koornneef, 2002; Lavagi et al., 2012).

Use of *Arabidopsis* as a model plant for abscission studies was first proposed by Bleeker and Patterson (1977). Although *Arabidopsis* plants do not abscise their leaves or flowers constitutively, floral organs are shed shortly after fertilization. Similar to traditional crop plant models for abscission, like tomato and bean, hormone treatment of *Arabidopsis* with ethylene or auxin promotes or inhibits abscission, respectively. These findings confirmed that the abscission process in *Arabidopsis* is compatible with other crop species (Bleeker and Patterson, 1997; van Doorn and Stead, 1997; Patterson, 2001). Since then, many scientists have used *Arabidopsis* to study abscission leading to a substantial molecular framework for abscission. These and future studies of abscission are of practical use for crop engineering while contributing to the basic understanding of plants (Tucker and Kim, 2015; Patharkar and Walker, 2017).

Abscission in *Arabidopsis* flowers is depicted in Figure 1.1. Following fertilization, floral organs senesce and abscise as a normal part of fruit development. The floral organs detach from specific AZs located at the base of floral organs on the flower receptacle. Figure 1.1 shows the location of sepal, petal, and stamen AZs. The abscission process can be divided into four stages: 1) AZ initiation, 2) competence to respond to abscission signals, 3) activation of abscission resulting in organ separation, and 4) differentiation of a protective surface layer over the scar (Estornell et al., 2013; Patharkar and Walker, 2017).

## 1.4 Step 1 – AZ initiation

As depicted in flowers, AZs typically form at the base of plant organs. These zones originate in the shoot apex during organogenesis. Every time a new organ is formed by the shoot apical meristem or floral meristem, a boundary region of low growth forms between the organ and the stem cell domain to keep these areas separated (Hepworth and Pautot, 2015). During organ enlargement, the boundary extends to encircle the base of the organ and has the potential to form an AZ (Hepworth and Pautot, 2015). Thus, AZ formation is concurrent with organ development (Patterson, 2001). AZs are four to six cell layers thick and contain small isodiametric cells with a dense cytoplasm (Sexton and Roberts, 1982; Roberts et al., 2002). A new detailed study reveals that AZs are differentiated into two cell types with distinct cellular activities. Cells located on the receptacle (named residuum cells) function as a separation layer that emits hydrolytic enzymes and cells located at the distal end of the floral organ (named secession cells) elaborate a lignified structure (2 to 3 layers of hexagonal-shaped cells with pillars) that is discarded with the organ (Lee et al., 2018). Newly exposed cells on the receptacle following abscission acquire epidermal fate leading to secretion of a protective cuticle over the scar (Lee et al., 2018). Boundary genes appear to play a role at several steps of the abscission process including AZ initiation, but the picture is far from clear (Hepworth and Pautot, 2015; Tucker and Kim, 2015; Patharkar and Walker, 2017).

### 1.4.1 *BLADE-ON-PETIOLE* genes

*BLADE-ON-PETIOLE 1/2* (*BOP1/2*) genes, first characterized in *Arabidopsis*, are conserved regulators of boundary patterning in land plants (Khan et al., 2014; Hepworth and Pautot, 2015). These genes are also essential for AZ initiation (McKim et al., 2008; Wu et al., 2012; Hepworth and Pautot, 2015; Couzigou et al., 2016; Xu et al., 2016). *BOP1/2* co-activator proteins are characterized by an N-terminal BTB/POZ (Broad-Complex, Tram track, and Bric-a-

brac/POX virus and zinc finger) domain located upstream of an ankyrin repeat domain (Khan et al. 2014). The BTB/POZ domain interacts with CULLIN3–RING E3 ubiquitin ligase (CRL3) to target transcription factors for degradation (Zhang et al., 2017; Chahtane et al., 2018). The ankyrin repeats interact with TGA (TGACG-motif binding) bZIP transcription factors for recruitment to DNA (Hepworth et al., 2005; Xu et al., 2010; Khan et al., 2014; Wang et al., 2018). BOP1/2 constitute a conserved subclade in the NON-EXPRESSOR OF PATHOGENESIS-RELATED GENES1 (NPR1) family of plant defense regulators. Distinct from *NPR1*, *BOP1/2* expression is enriched at organ boundaries, such that loss-of-function mutations strongly impact the morphology of leaf petioles and flowers (Hepworth et al., 2005; Khan et al., 2014). In flowers, *BOP* genes are expressed in young emerging floral organs and quickly localize to the base where they act at the earliest stages of AZ initiation. AZs fails to form in *bop1 bop2* flowers causing permanent attachment of floral organs to the base of the fruit (McKim et al., 2008). *BOP1/2* expression continues in the AZ until fruits are mature hinting at additional roles in later steps of the abscission process (McKim et al., 2008; Xu et al., 2010).

#### **1.4.2 TGA bZIP genes**

TGA bZIP transcription factors recruit BOP1/2 proteins to DNA (Hepworth et al., 2005; Xu et al., 2010; Wang et al., 2018). The Arabidopsis genome contains ten TGA genes grouped into five subclades (clade I: *TGA1* and *TGA4*; clade II: *TGA2*, 5, and 6; clade III: *TGA3* and *TGA7*; clade IV: *TGA9* and *TGA10*; and clade V: *TGA8*, also known as *PERIANTHIA/PAN*) (Gatz, 2013). In flowers, BOP1/2 proteins interact with clade V TGA8/PAN to regulate the number and arrangement of floral organs. Flowers of *bop1 bop2* and *tga8* mutants contain a similar fifth organ in the sepal whorl (Hepworth et al., 2005; Xu et al., 2010). Clade I *TGA1* and *TGA4* genes are expressed in organ boundaries and function in the same genetic pathways as *BOP1/2*. Recent work

shows their importance for meristem maintenance, flowering and inflorescence architecture (Wang et al., 2018). Clade I TGA transcription factors are essential for BOP1-dependent induction of *ARABIDOPSIS THALIANA HOMEODOMAIN GENE1 (ATH1)*, a boundary gene required for abscission (Gómez-Mena and Sablowski, 2008; Wang et al., 2018). Despite this interaction, *tga1 tga4* mutants have no obvious abscission defects suggesting compensation by other TGA factors (Wang et al., 2018).

### **1.4.3 TALE homeobox genes**

Three-amino-acid-loop-extension (TALE) homeodomain transcription factors are characterized by an insertion of three amino acids in the loop connecting  $\alpha$ -helices 1 and 2 in the homeodomain (Bürglin, 1997). Plant TALE transcription factors include KNOTTED1-like (KNOX) and BEL1-like (BELL or BLH) members which function as heterodimers (Hamant and Pautot, 2010). In inflorescences, BOP1/2 co-activators require the downstream activity of at least two boundary TALE factors: the BELL-like member ATH1 and its KNOX binding partner KNOTTED-LIKE FROM ARABIDOPSIS THALIANA6 (KNAT6), whose activity is partially redundant with KNAT2 (Belles-Boix et al., 2006; Rutjens et al., 2009; Li et al., 2012; Khan et al., 2012a; Khan et al., 2012b). *knat2* and *knat6* mutations do not obviously disrupt boundary patterning on their own but *KNAT6* contributes with *SHOOT MERISTEMLESS* to meristem initiation and organ separation (Belles-Boix et al., 2006). The inactivation of *KNAT2* and *KNAT6* causes slightly delayed organ abscission (Belles-Boix et al., 2006; Shi et al., 2011). Boundary defects in *ath1* mutants are more severe (Gómez-Mena and Sablowski, 2008). The stamens in *ath1* mutants are partially fused and stamen AZ formation is impaired resulting in delayed abscission of mainly stamens (Gómez-Mena and Sablowski, 2008). These data suggest a potential role for boundary TALE genes in AZ initiation.

## **1.5 Step 2 - AZ cells acquire competency to react to signals**

After AZ initiation, AZ cells become competent to respond to signals for abscission. Competence is associated with withering of floral organs upon fertilization. This process involves a decline in auxin, thought to sensitize AZ cells to ethylene which accelerates abscission (Taylor and Whitelaw, 2001; Meir et al., 2015). Abscisic acid and jasmonic acid are also positive signals for abscission (Estornell et al., 2013; Kim, 2014). Developmental regulators that impart competence to respond to abscission signals remain unclear. Members of the MADS-box gene family are suggested to play a role (Patharkar and Walker, 2017).

### ***1.5.1 MADS-box genes***

The MADS-box genes belong to a large and diverse family in plants. The MADS box is a conserved sequence that encode a DNA binding domain known as the MADS domain, consisting of 55 to 60 amino acids. Members are found in all eukaryotic organisms. In plants, this family has another less conserved protein-protein interacting domain, known as the K domain (Ng and Yanofsky, 2001). *AGAMOUS-LIKE 15 (AGL15)*, *AGL18*, and *FOREVER YOUNG FLOWER (FYF/AGL42)* are members of this family that potentially play a role in AZ competency (Fernandez et al., 2000; Kim, 2014; Patharkar and Walker, 2017). When these genes are overexpressed, abscission is delayed but AZ anatomy is not altered. MADS-box transcription factors might control the timing of abscission by acting as negative regulators (Fernandez et al., 2000; Adamczyk et al., 2007; Chen et al., 2011). A recent study showed that *AGL15* represses the transcription of receptors required for activation of abscission thereby inhibiting their premature signaling. This repression is relieved by phosphorylation of *AGL15* upon activation of abscission (Patharkar and Walker, 2015).

## 1.6 Step 3 - activation of abscission

Activation of abscission causes the induction of enzymes in the separation layer that dissolve the cell wall and attachments between cells in the fracture plane of the AZ (Estornell et al. 2013; Dong & Wang 2015). Major enzyme classes contributing to cell wall loosening are expansins, pectinases, glucanases, polygalacturonases, and xyloglucan hydrolases (Roberts et al., 2002; Estornell et al., 2013). Receptor-ligand mediated signaling plays an important role in activating the production of these enzymes (Dong and Wang, 2015; Patharkar and Walker, 2017).

### 1.6.1 IDA signaling pathway

Activation of abscission relies on two functionally redundant receptor-like protein kinases HAESA (HAE) and HAESA-LIKE2 (HSL2) on the cell surface. A *hae hsl2* double mutant shows no abscission of floral organs (Jinn et al., 2000; Cho et al., 2008; Stenvik et al., 2008). HAE/HSL2 receptors form one half of a complex with SOMATIC EMBRYOGENESIS RECEPTOR-LIKE KINASE 1/2/3/4 (SERK1/2/3/4) (Meng et al., 2016; Santiago et al., 2016). SERK3, also known as BRI1-ASSOCIATED RECEPTOR KINASE 1 (BAK1) was previously identified as a co-receptor for BRASSINOSTEROID INSENSITIVE 1 (BRI1). BRI1 is the receptor that perceives brassinosteroid hormones, responsible for cell expansion and elongation (He et al., 2000). BAK1 was also previously identified as a co-receptor for FLAGELLIN-SENSITIVE 2 (FLS2). FLS2 is the receptor that perceives bacterial flagellin, responsible for activation of innate immunity (Gómez-Gómez and Boller, 2000; He et al., 2000; Nam and Li, 2002). Transcripts induced by abscission signaling significantly overlap with plant innate defense genes, possibly accounting for overlap between HAE/HSL2 and SERK-type receptor functions (Chris Bergin, M.Sc. thesis).

The ligand for HAE/HSL/SERK receptors is encoded by the *INFLORESCENCE DEFICIENT IN ABSCISSION (IDA)* gene (Santiago et al., 2016). This gene was identified as a

mutation in Arabidopsis that blocks floral organ abscission. The IDA protein is processed by cleavage to create a bioactive peptide of 14 amino acids (Butenko et al., 2003; Schardon et al., 2016). Binding of this secreted IDA peptide appears to stabilize a protein complex between HAE/HSL2 and SERK1/2/3/4 at the membrane, based on studies in Arabidopsis leaf protoplasts and tobacco epidermal cells (Meng et al., 2016; Santiago et al., 2016). Consistent with these data, overexpression of *IDA* causes significant enlargement of the AZ and early abscission which is reversed by a knockout of *HAE/HSL2* (Stenvik et al., 2006; Cho et al., 2008).

Receptor activation by IDA ligand induces a MITOGEN-ACTIVATED PROTEIN KINASE (MAPK) cascade which consists of MKK4/5 and MPK3/6 (Cho et al., 2008). Constitutively active mutant forms of MKK4/5 restore abscission in *hae hsl2* double mutants indicating that these kinases function genetically downstream of the receptor complex (Cho et al., 2008). Activation of the MAPK kinase cascade leads to expression of hydrolytic enzymes for abscission (Cho et al., 2008).

Interestingly, genetic and expression analyses show that antagonistic interactions between TALE members that control inflorescence architecture also govern the timing of abscission (Ragni et al., 2008; Shi et al., 2011; Zhao et al., 2015). Activation of the IDA signalling pathway downregulates the activity of KNOX transcription factor BREVIPEDICELLUS (BP/KNAT1) in AZs leading to an increase of *KNAT2* and *KNAT6* expression, which act as positive regulators of floral organ separation (Shi et al., 2011). BP directly represses boundary genes *KNAT2* and *KNAT6* (Zhao et al., 2015) whose increase in the AZ directly or indirectly activates genes involved in cell separation since *knat2 knat6* mutants respond more slowly to signals for abscission. Double mutations in *KNAT2* and *KNAT6* also suppress the early abscission phenotype of plants that overexpress *IDA* and suppress the early abscission phenotype of *bp*, with *bp knat2 knat6* triple

mutants exhibiting a slight delay in abscission similar to *knat2 knat6* mutants (Shi et al., 2011). Previous studies in inflorescences also show an antagonistic interaction between BP and ATH1, which is a functional partner of KNAT2 and KNAT6 (Rutjens et al., 2009; Li et al., 2012; Khan et al., 2012a). This suggests that ATH1 which plays a role in AZ initiation might also contribute to activation of abscission.

The abscission process relies heavily on the membrane trafficking for controlling the abundance of cell surface receptors and secretion of separation enzymes. Mutations in an ADP-ribosylation factor GTPase-activating protein NEVERSHED (NEV) block abscission. The structure of Golgi cisternae and movement of transport vesicles is disrupted in *nev* mutants (Liljegren et al., 2009). Various suppressors of the *nev* phenotype have been identified, including mutations in *EVERSHED (EVR)* which encodes a receptor-like protein kinase (Leslie et al., 2010), *CAST AWAY (CST)* which encodes a receptor like cytoplasmic protein kinase (Burr et al., 2011), and *SERK1* which is part of the HAE/HSL2 receptor complex (Lewis et al., 2010). How mutations in *EVR/CST/SERK1* rescue the *nev* mutant phenotype is unexplained. Mutations in all three genes cause the disorganization of separation/epidermal cells in the AZ scar region resulting in a morphology similar to IDA overexpression lines (Stenvik et al., 2006). These findings suggest that players responsible for abscission might also function in the final differentiation of protective epidermal cells over the AZ scar.

### ***1.6.2 Mechanics of separation***

The AZ contains two distinct cell types that guide precise separation between the cell layers during floral organ abscission (Lee et al., 2018). The separation layer is comprised of residuum cells that remain attached to the plant body after abscission. Cells in this layer secrete hydrolytic enzymes for cell separation. The lignified layer is composed of secession cells that remain with

the base of discarded organs. At the base of separating organs, cell margins are lignified to form a hexagonal network with pillars. The honeycomb structure acts as a brace in holding the layers of separating cells together. The lignified layer has a second role in limiting the diffusion of hydrolytic enzymes from the separation layer. A barrier of lignin constrains the fracture plane of organs to central cells in the AZ allowing a precise organ separation and ensuring the surface integrity of receptacle epidermal cells (Lee et al., 2018).

### **1.7 Step 4 - differentiation of a protective layer**

Once an organ is shed, the newly exposed surface on the plant body is sealed to protect against water loss and colonization by pathogens (Estornell et al., 2013). The composition of this protective layer is debated. Substances including suberin, lignin, waxes, reactive oxygen species (ROS), and/or defense-related proteins are thought to play a role. Many of these substances are not solely produced following organ abscission but begin to be accumulated during the third step of abscission (Roberts et al., 2000; Meir et al., 2011; Kim, 2014). Transcript profiling of residuum receptacle cells in *Arabidopsis* suggests that the protective layer is made of cuticle. Thus, newly exposed separation layer cells on the plant body may acquire epidermal cell identity for the synthesis of cuticle (Lee et al., 2018).

### **1.8 Thesis rationale**

Boundaries provide a point of attachment of organs to the plant body. However, knowledge of how boundary genes contribute to the abscission process is fragmented. A model is presented in Figure 1.2. AZ formation requires *BOP1/2* (McKim et al., 2008; Lee et al., 2018) and to a lesser extent *ATH1* (Gómez-Mena and Sablowski, 2008) but other members involved in this step are unknown. Boundary TALE homeobox genes are good candidates. In inflorescences, BOP1/2 co-activators require the downstream activity of at least two boundary TALE factors: the BELL-like

member ATH1 and its KNOX binding partner KNAT6, whose activity is partially redundant with KNAT2 (Belles-Boix et al., 2006; Ragni et al., 2008; Rutjens et al., 2009; Li et al., 2012; Khan et al., 2012a; Khan et al., 2012b; Khan et al., 2015). Abscission is slightly delayed in *ath1* single mutants and *knat2 knat6* mutants respond more slowly to abscission signals resulting in slight retention of floral organs (Gómez-Mena and Sablowski, 2008; Shi et al., 2011). Continuous expression of boundary genes in the AZ of flowers and fruits hints at an involvement throughout the abscission process (McKim et al., 2008; Ragni et al., 2008). In support of this model, epistasis and expression analyses show that KNAT6 and to a lesser extent KNAT2 function downstream of IDA signaling to promote organ detachment (Shi et al., 2011). My project was designed to further examine how boundary genes contribute to the abscission process.

My thesis directly tests the following hypotheses:

1. TALE homeobox genes contribute to the formation of AZs.
2. Boundary genes are collectively required for organ separation.

My thesis examines the contribution of *ATH1*, *KNAT2*, and *KNAT6* genes to the formation of AZs. I also examine the impact of TGA factors in abscission since BOP1/2 work in concert with these transcription factors. Finally, I begin to explore whether BOP1/2 and ATH1 contribute to organ separation at the same step as KNAT and KNAT6.

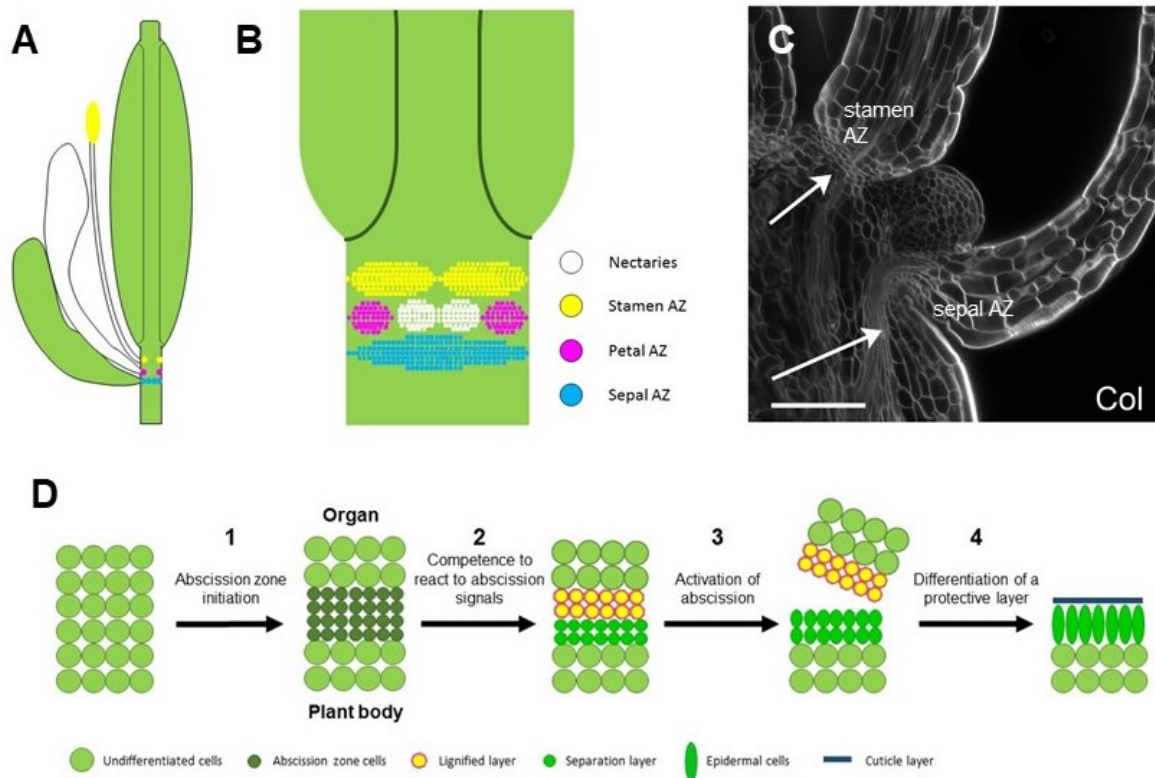


**Figure 1.1 Arabidopsis flower abscission zones and model for abscission.**

A-B, Schematic representation of the position of AZs in Arabidopsis flowers. Colours denote sepals (blue), petals (purple), stamens (yellow), and nectaries (white). A, Mature flower showing AZs at the base of floral organs. B, Schematic representation of the sepal, petal, and stamen AZ organization on the receptacle after organ detachment. C, Confocal section of a wild type flower at anthesis (stage 13) showing the sepal and stamen AZs consisting of small cells. Image by Véronique Pautot. Scale bar, 100  $\mu\text{m}$ . D, The current accepted model of abscission proposes a four-step process beginning with the initiation of an AZ that matures to form a separation layer that emits hydrolytic enzymes and a lignified layer that acts as a mechanical brace. Activation of abscission leads to dissolution of the middle lamella midway through the AZ. The last step of abscission involves the differentiation of a protective epidermal layer over exposed cells on the surface of the floral receptacle.

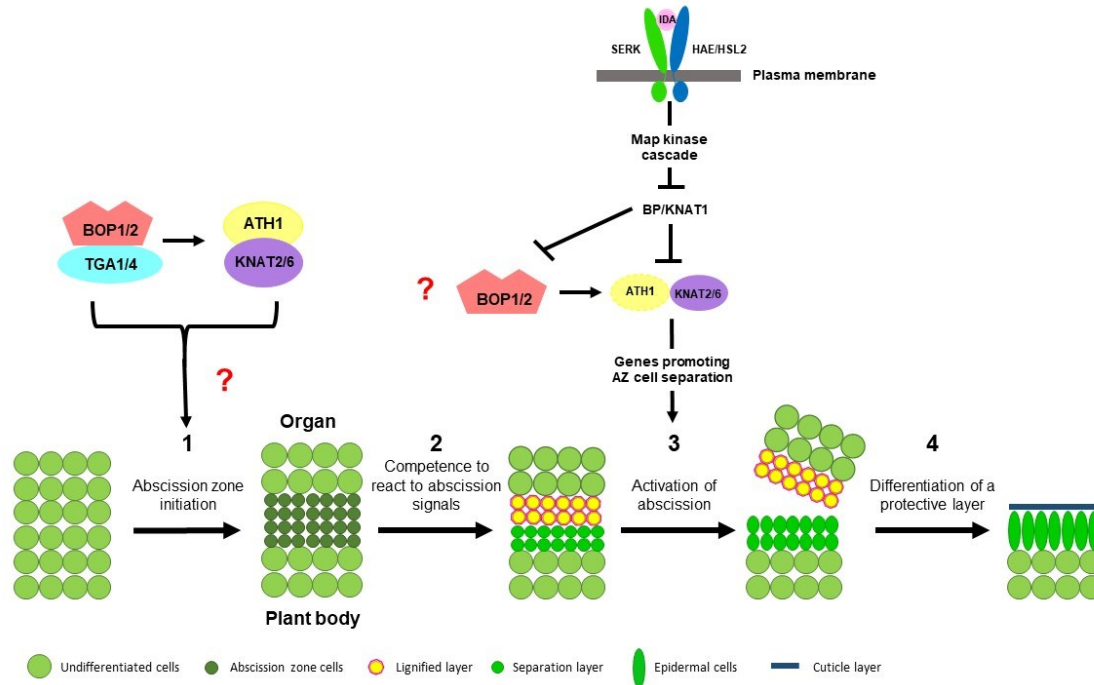


**Figure 1.2 Schematic representation of thesis hypothesis.**

Abscission is a four step process beginning with the initiation of an AZ. In response to fertilization, AZ cells acquire competence to respond to abscission signals leading to the activation of IDA signaling. Transduction of this signal results in organ separation. Newly exposed cells on the plant body undergo differentiation to form a protective layer over the scar. My thesis examines the role of boundary genes in this four-step process. BOP1/2 co-activator proteins interact with clade I TGA1 and TGA4 transcription factors to directly and indirectly promote the expression of TALE homeobox genes *ATH1* and *KNAT6* which are important for boundary patterning. How this module contributes to abscission is only partly understood. BOP1/2 are essential for AZ initiation. My work tests the hypothesis that boundary TGA bZIP and TALE homeodomain transcription factors also contribute to this step. My work also tests the hypothesis that boundary genes from this module function downstream in the IDA signaling pathway to promote organ separation.

## CHAPTER 2 : MATERIALS AND METHODS

### 2.1 Plant material and growth conditions

The Columbia-0 (Col-0) ecotype of *Arabidopsis thaliana* was used as wild type (WT). Mutant alleles of *ath1-3* (Gómez-Mena and Sablowski, 2008), *kmat2-5*, *kmat6-1* (Belles-Boix et al., 2006), *bp-2* (introgressed from RLD into Col-0) (Venglat et al., 2002), *bop1-3*, *bop2-1* (Hepworth et al., 2005), *tga1-1* and *tga4-1* (Kesarwani et al., 2007) were as previously described. The *BOPI* overexpression (*BOPI o/e*) line used in this study is *bop1-6D*, an activation-tagged gain-of-function mutant with four viral 35S enhancer copies in the 5' control region of *BOPI* resulting in high constitutive levels of expression (Norberg et al., 2005). The *ATH1:GUS* reporter line used this study has also been previously described (Proveniers et al., 2007; Woerlen et al., 2017). All mutant combinations were constructed by crossing and confirmed by PCR genotyping. Table 2.1 is a list of genetic materials used in this study.

Seeds were surface sterilized with 100% ethanol followed by a solution of 5% hypochlorite (bleach) and 0.5% (w/v) sodium dodecyl sulphate. Following this treatment, seeds were rinsed 2-4 times in sterile distilled water and sown on agar plates containing minimal media (Haughn and Somerville, 1986). Plates were incubated in the dark for 2 days at 4°C to break dormancy. Seeds were germinated at 22°C in a growth chamber under long days (16 h light/8 h dark) or continuous light (24 h light/0 h dark) as required. One-week-old seedlings were transplanted to sterilized soil (Promix BX, Premier Horticulture, Rivière-du-Loup, QC) supplemented with a 1 g L<sup>-1</sup> solution of 20-20-20 plant fertilizer (Plant-Prod Inc., Brampton, ON) and grown to maturity. Phenotypic assays were performed on 6-week-old plants with a minimum of 16 siliques on the primary inflorescence.

## 2.2 Extraction of genomic DNA and genotyping

Genomic DNA was extracted as described (Edwards et al., 1991) with minor modifications. From each plant, a young rosette leaf (about the size of a thumbnail) was placed in a 1.5 ml microcentrifuge tube and ground to a paste using a pellet pestle. A 400  $\mu$ L aliquot of DNA extraction buffer (200 mM Tris-HCl pH 7.5, 250 mM NaCl, 25 mM EDTA pH 8.0, 0.5% w/v SDS) was added to the tube, vortexed for 5 sec, and then centrifuged for 10 min at 13,000 g. A 350  $\mu$ L aliquot of the resulting supernatant was transferred to a new tube containing 400  $\mu$ L of isopropanol for precipitation of genomic DNA. The tubes were immediately inverted five times and then left at room temperature for 10 to 15 min. The tubes were centrifuged for another 10 min to collect the DNA. The supernatant was discarded, and the pellet was washed with 800  $\mu$ L of 80% ethanol. The final pellets were then left to air-dry until all the ethanol was evaporated. The pellet was dissolved in 100  $\mu$ L of TE buffer pH 7.0 and the tubes were stored at 4°C. Two  $\mu$ L of the DNA prep was used as template in a standard 20  $\mu$ L PCR-genotyping reaction.

Table 2.2 lists primers used for genotyping. T-DNA insertion mutants from the SALK collection were genotyped as described ([www.signal.salk.edu](http://www.signal.salk.edu)). The *bp-2* mutant was genotyped as previously described (Khan et al., 2012b).

## 2.2 Scanning electron microscopy (SEM)

SEM samples were prepared as previously described (Modrusan et al., 1994) with minor modifications. Sepals, petals, and stamens of flowers were dissected to observe the AZ, as required. Tissues were fixed overnight at 4°C in a solution of 3% glutaraldehyde in 0.1 M sodium phosphate buffer pH 7.0. One or two drops of Triton X-100 were added per 5 ml of buffer to reduce surface tension. The next day, the fixative was removed, and the samples were washed twice with 0.1 M sodium phosphate buffer pH 7.0. The samples were then post-fixed in 1% osmium tetroxide

in 0.05 M sodium phosphate buffer pH 7.0 for two hours. After treatment, the samples were washed three times with 0.1 M sodium phosphate buffer pH 7.0 and dehydrated using a graded ethanol series (30%, 50%, 70%) for 30 min each. Samples were stored in 70% ethanol for up to three weeks until critical point drying. Just before, the samples were further dehydrated for 30 minutes in 90% ethanol followed by two changes of 100% anhydrous ethanol (stored over molecular sieves). The samples were then placed in a critical point dryer (EMITECH, K850) which exchanges ethanol for carbon dioxide. The dried samples were mounted on aluminum stubs and coated with gold-palladium using a turbo-pumped sputter coater (Quorum tech, Q150T ES). The prepared samples were then imaged using an SEM (Vega-II XMU, Tescan) at an accelerating voltage of 15kV. Images were taken at 40X and 238X magnification. Image J software version 1.52e was used to measure the length of the medial and lateral AZs from SEM images (<https://imagej.nih.gov/ij/notes.html>). The medial and lateral AZs were measured at three locations per silique, while ensuring to incorporate all three AZs (sepal, petal, and stamen) using a minimum of four siliques per genotype. Student t-tests were performed to identify the significances of these results in comparison to wild type.

### **2.3 Petal break strength**

Petal break strength quantifies the force required to remove a petal from the receptacle. Petal break strength was measured using an apparatus similar to Lease et al. (2006). To assess break strength, we used a custom built load cell apparatus and a custom built DC amplifier. The load cell was operated as a cantilevered beam – it was fixed at one end and the applied force deflected the unfixed end. The load cell was comprised of four 102 ohm resistive strain gauge elements (Micro-Measurements, Raleigh, NC) with two elements fixed to the upper, and two elements fixed to the lower surfaces of a 0.036 inch (0.90 mm) fiberglass board measuring 3.15

inches (80 mm) long by 0.63 inches (16 mm) wide. The strain gauge elements were fixed on each side with epoxy resin in a “T” configuration at the centre of the described fiberglass board. The length of this board was extended by affixing an additional 4 inch (102 mm) by 0.36 inch (9 mm) length of 0.036 inch (0.9 mm) thick fiberglass board. The extension of the first board in this manner increased the overall sensitivity of the load cell (acting as a ‘mechanical’ amplifier). A spring-type electronics ‘hook’ test probe (Pomona, Model 3925) was fixed to the end of the load cell and allowed individual petals to be grasped.

The output of the amplifier (load cell output) was calibrated by placing known loads (50, 100, 200, 500, 1000, 2000 and 5000 mg) (calibration weight kit, class M2, American Weigh Scales) on the load cell at the location of the hook used for grasping petals. Because the load deflected the load cell arm under the influence of gravity, force was calculated simply as mass (kg) multiplied by acceleration due to gravity ( $9.81 \text{ m}\cdot\text{s}^{-2}$ ). The voltage output of the amplifier, measured with a multimeter (Agilent, model U1233A), was linear over the range of measurements taken.

To take a petal break strength measurement, a petal was placed in the gripper and put under minor manual tension until the stem was straight. The voltmeter was then zeroed, and the stem of the plant was manually pulled using even force until the petal was detached from the flower. The voltage output after petal detachment was then used to calculate force in millinewtons using the standard curve. Petal break strength was measured for 2 petals per flower at every other position beginning at position 2 and ending at abscission or position 16. For each break event, it was checked that a petal was in the gripper, as confirmation that the petal did not slip out or tear inappropriately during the assay. A ANOVA test was performed to identify the significant differences between each mutant at every position.

## 2.4 Localization of GUS activity

Detection of  $\beta$ -glucuronidase (GUS) activity was carried out as previously described (Khan et al., 2012b) with minor modifications. Fresh tissue was added to 90% acetone fixative chilled on ice. When collection was complete, samples were warmed to room temperature for 15 min, the acetone was removed, and samples were submerged in staining solution containing 5 mM  $K_3Fe(CN)_6$ , 5 mM  $K_4Fe(CN)_6$ , and 2 mM 5-bromo-4-chloro-3-indoxyl- $\beta$ -D-glucuronide (X-Gluc). Samples were incubated at 37°C until a localized blue precipitate was visible (3 to 24 hours). Samples were cleared in 70% ethanol and imaged with a digital camera under a stereomicroscope (SteRIO Discovery V20 with Axiocam, Carl Zeiss).

**Table 2.1: List of genetic materials used in this study**

<b>Plant line</b>	<b>Description</b>	<b>Annotation</b>	<b>Reference</b>
<b><u>Loss-of-function mutants</u></b>			
<i>bop1-3</i>	T-DNA insertion	SALK_012994	Hepworth et al., 2005
<i>bop2-1</i>	T-DNA insertion	SALK_075879	Hepworth et al., 2005
<i>tga1-1</i>	T-DNA insertion	SALK_028212	Kesarwani et al., 2007
<i>tga4-1</i>	T-DNA insertion	SALK_127923	Kesarwani et al., 2007
<i>ath1-3</i>	T-DNA insertion	SALK_113353	Gómez-Mena and Sablowski, 2008
<i>knat2-5</i>	T-DNA insertion	SALK_099837	Belles-Boix et al., 2006
<i>knat6-1</i>	T-DNA insertion	SALK_047931	Belles-Boix et al., 2006
<i>bp-2</i>	C to T transition, creates stop codon at position 540	RLD ecotype, backcrossed 3X to Col-0	Venglat et al., 2002
<b><u>Gain-of-function mutant</u></b>			
<i>bop1-6D</i>	Activation tagged line, 4X CaMV 35S enhancer in <i>BOP1</i> promoter	Glufosinate-ammonium selection in plants (active)	Norberg et al., 2005
<b><u>GUS reporter line</u></b>			
<i>ATH1:GUS</i>	2.6-kb genomic fragment of <i>ATH1</i> containing 1.3-kb of promoter sequence, 5' UTR, and first 42 amino acids of coding sequence fused in-frame to GUS	Kanamycin selection in plants (inactive)	Proveniers et al., 2007

**Table 2.2: List of primers used for genotyping**

<b>Allele</b>	<b>Primers</b>	<b>Sequence (5' to 3')</b>	<b>Reference</b>
<i>bop1-3</i>	bop1-3 SALK_012994 RP	TGACATCGGAGAAAGCTTGAC	Hepworth et al., 2005
	bop1-3 SALK_012994 LP	TGCACAATCTTTCGACTTCATC	
<i>bop2-1</i>	bop2-1 SALK_075879 RP	ATTTGGCCCACCTTTGTATTC	Hepworth et al., 2005
	bop2-1 SALK_075879 LP	AAAGAGAGAACCTGGGTGAGC	
<i>knat6-1</i>	knat6-1 LP	GAAGATAAACCTAGCTACAAG	Pautot (unpublished)
	knat6-1 RP	ATATCAGTAAACCACAAAGAAAGTC	
<i>ath1-3</i>	ath1 RP	GGCGGGTTTCGGATCTACATT	Gómez-Mena and Sablowski, 2008
	ath1 LP	CCAATACCGGTTTTTCAGACATGA	
<i>knat2-5</i>	kn2-5 RP-2	TTCAACCACCGGAGACAATCAAAGA	Hepworth (unpublished)
	kn2-5 LP-2	TGTAGCAGACGCTGGACCAGTGAC	
<i>bp-2</i>	bp-2 dCAPs F1	ACCCTCCTACAAGCTTACTTGGACTGCCA	Khan et al., 2012b
	bp-2 dCAPs R1	GGAGGCAGAGACAGACGGTGTTGACCGCT	
<i>tga1-1</i>	tga1 salk_028212 RP	TAGGGAATCTCCGTGTCCCCTCTCG	Khan et al., 2015
	tga1 salk_028212 LP	TTCAAAACCTGGATTCATGGTTTCC	
<i>tga4-1</i>	tga4-1 SALK_127923 RP	GAAGGTTTGAAGTTTACGAGCCTCT	Wang et al., 2018
	tga4-1 SALK_127923 LP	GCTCTGCTGAAGTTTTCCACATTCC	

## CHAPTER 3 : RESULTS

### 3.1 Progressive loss of ATH1, KNAT6 and KNAT2 activity impairs boundaries in flowers

BOP1/2 are required for AZ formation but how they promote differentiation of these cell layers is unknown. In inflorescences, BOP1/2 require the downstream activity of TALE transcription factors ATH1 and KNAT6 for patterning boundaries. ATH1 is a BELL-like member that interacts with KNAT6 and KNAT2, two closely related KNOX factors, also expressed at boundaries. Mutations in *ATH1* cause a delay in stamen AZ initiation (Gómez-Mena and Sablowski, 2008). The *knat2 knat6* mutant also shows a mild delay in abscission suggesting that these factors might collectively contribute to AZ initiation. To test this hypothesis, we first examined the effect of their progressive loss-of-function on boundary patterning in the flower. Double and triple mutants were generated by crossing *ath1* mutants to *knat2* and *knat6* single mutants and *knat2 knat6* double mutants. Mutant combination flowers were examined by SEM for defects in boundary morphology in parallel with wild type, *bop1 bop2*, and *ath1* control flowers (Figure 3.1). In wild type flowers, the sepals were well-separated and boundaries were distinct, whereas *bop1 bop2* flowers showed occasional fused sepals (1/3 flowers had a sepal fusion). The sepal-sepal fusion defect was more frequent in *ath1* flowers (2/5 flowers had fusions). Floral organ fusions became increasingly severe in *ath1 knat2*, *ath1 knat6*, and *ath1 knat2 knat6* mutants, with flowers showing fusions within and between whorls. Flowers of these mutants had also defects in the boundary that separates sepals from the floral pedicel. Boundaries at the base of *ath1* flowers were smoothed (Gómez-Mena and Sablowski, 2008 and this work). This defect was enhanced with the progressive inactivation of *KNAT2* and *KNAT6* with *ath1 knat2 knat6* flowers lacking boundaries. Sepal fusions were also observed in *knat2 knat6* double mutants but not in *knat2* and *knat6* single mutant flowers (Supplementary Figure S1). These data confirmed a dominant role for

*ATH1* in patterning flower boundaries and showed a contribution for *KNAT6* and to a lesser extent *KNAT2*.

### 3.2 Progressive loss of *ATH1*, *KNAT6*, and *KNAT2* activity impairs floral organ abscission

AZ formation is blocked in *bop1 bop2* double mutants (McKim et al., 2008). To further determine the impact of *ATH1*, *KNAT6*, and *KNAT2* in abscission, the process was monitored in inflorescences from wild type, *bop1 bop2*, and *ath1* control plants in parallel with *ath1 knat2*, *ath1 knat6*, and *ath1 knat2 knat6* combination mutants. The convention to stage abscission is to label the youngest flower with visible white petals as position 1. Older flowers on the inflorescence are numbered consecutively (Bleeker and Patterson, 1997). Qualitative and quantitative phenotypic analyses were performed on  $n \geq 20$  plants per genotype (Figure 3.2 and Supplemental Table S1). Floral organs in wild type abscised between positions 5 and 7 (position  $6.4 \pm 0.2$ ) whereas floral organs in *bop1 bop2* stayed firmly attached. Analysis of mutant combinations with *ath1* showed that mild abscission defects in *ath1* were progressively enhanced by *knat2*, *knat6*, and *knat2 knat6* mutations. *ath1* mutants showed a slight delay in floral organ abscission (position  $9.0 \pm 0.2$ ) with mainly prolonged attachment of stamens as previously reported (Gómez-Mena and Sablowski, 2008). Abscission was further delayed in *ath1 knat2* mutants (position  $12.1 \pm 0.4$ ) while *ath1 knat6* and *ath1 knat2 knat6* triple mutants retained their floral organs for the entire life span (Figure 3.2 and Supplemental Figure S2). Floral organs in *knat2 knat6* mutants were slightly retained but detachable by gentle touch (Supplemental Table S1) as previously reported (Shi et al., 2011).

Petal break strength refers to the amount of force required to remove a petal from the receptacle of the flower (Craker and Abeles, 1969). To further quantify defects in abscission, petal break strength was measured using a petal break strength meter (Lease et al., 2006). In wild type plants, a gradual decline in petal break strength is initiated at fertilization owing to the progressive

degradation of the middle lamella in the AZ (McKim et al., 2008). Figure 3.3 shows that in wild type, *ath1*, and *ath1 knat2* mutants, there was a gradual decline in petal break strength between positions 2 and 16. By contrast, little or no decline was observed in *bop1 bop2*, *ath1 knat6*, and *ath1 knat2 knat6* mutants. These data are consistent with a defect in either formation of the AZ or the separation process.

To further distinguish between these possibilities, SEM was used to examine the receptacles of wild type and mutants (Figure 3.4). Petals were forcibly removed to expose the AZ as required. Wild type fracture planes show a progression from broken cells (position 2 and 4) to rounded AZ cells (position 6 and higher). In *bop1 bop2*, fracture planes at all positions showed broken cells indicating that AZs were not formed. In *ath1* and *ath1 knat2* mutants, the formation of rounded AZ cells was delayed (position 8) and the stamen AZ was expanded and disorganized (position 10 and 12). There was some variation in the severity of the *ath1* abscission defect between experiments, ranging from mildly disrupted AZs to more severe disruption as depicted in Figure 3.4. Measurements showed that AZ enlargement in *ath1* mutants was primarily along the medial axis (Supplemental Figure S3). In *ath1 knat6* and *ath1 knat2 knat6* mutants, the floral AZs were severely disorganized and expanded along both medial and lateral AZ axes (Figure 3.4 and Supplemental Figure S3). In *ath1 knat2 knat6* triple mutants, broken cells were still evident at position 8, showing a defect in AZ initiation. At higher positions, organs in *ath1 knat6* and *ath1 knat2 knat6* were cleanly detached at the AZ, but only by strong force, suggesting a problem in the separation process. In contrast to *ath1* double and triple mutants, the receptacle AZs of *knat2*, *knat6*, and *knat2 knat6* mutant flowers were only slightly expanded (Supplemental Figure S4). Confocal images also showed a delay in AZ initiation in *ath1* flower boundaries that is dramatically aggravated in the absence of *KNAT6* and *KNAT2* (Supplemental Figure S5). These

collective data confirm that ATH1 plays a dominant role in initiation of AZs and reveals a contribution for KNAT6 and to a lesser extent KNAT2. Therefore, besides their role in organ separation, KNAT6 and KNAT2 contribute to AZ initiation with ATH1 by preventing cell growth and proliferation.

### 3.3 Clade I TGAs contribute to AZ formation

BOP1/2 proteins interact with clade I TGA factors via their ankyrin repeats. This interaction is important for BOP1 recruitment to TGA binding sites in the *ATH1* promoter (Wang et al., 2018). Clade I *TGAI* and *TGA4* genes are strongly expressed in the AZ of flowers, but *tgal tga4* double mutants have no obvious abscission defects (Wang et al., 2018). Double mutant analysis was used to test if clade I TGAs are partially required for abscission. Higher order mutants were obtained by crossing *ath1* mutants to *tgal*, *tga4*, and *tgal tga4* mutants. The resulting genotypes were analyzed for floral and abscission defects (Figure 3.5). SEM imaging showed phenotypically normal flowers for *tgal tga4* and a similar number of mild sepal fusions in *ath1*, *ath1 tgal*, *ath1 tga4*, and *ath1 tgal tga4* mutant flowers. The timing of abscission in *ath1* mutants was similar to *ath1 tgal*, *ath1 tga4*, and *ath1 tgal tga4* mutants. Analysis of petal break strength supported this finding (Figure 3.6). However, SEM analysis portrayed increasing disorganization of AZs in *ath1 tgal*, *ath1 tga4*, and *ath1 tgal tga4* triple mutants compared to the *ath1* single mutant (Figure 3.7). In *ath1*, only the stamen AZs were significantly disorganized. The additional loss of *TGAI*, *TGA4*, and *TGAI TGA4* resulted in further disorganization of sepal and petal AZs. These data support a partial role for clade I TGAs in abscission, likely in the same pathway as BOP1/2 and ATH1. Thus, *tgal tga4* mutations enhance *ath1* AZ proliferation defects without blocking abscission. These data suggest that other TGA transcription factors or other transcription factors are involved.

### 3.4 *ATH1* functions downstream of BP

IDA signaling promotes abscission (Patharkar and Walker, 2017). Activation of this pathway inhibits BP/*KNAT1*, a direct repressor of *KNAT2* and *KNAT6* boundary genes (Shi et al., 2011; Zhao et al., 2015). In *bp* mutants, the fruits are downward pointing (Figure 3.9E). This phenotype is caused by upregulation of *KNAT2* and *KNAT6* in pedicels leading to localized restriction of growth below nodes and downward pointing fruits (Ragni et al., 2008; Li et al., 2012; Khan et al., 2012a; Khan et al., 2012b). Besides these defects, the AZ region in *bp-3* fruits is expanded towards the pedicel region and abscission occurs about one position earlier than wild-type (Shi et al., 2011). These *bp-3* defects are rescued by inactivation of *KNAT2* and *KNAT6* except that abscission is weakly delayed in *bp-3 knat2 knat6* triple mutants, similar to *knat2 knat6* mutants (Shi et al., 2011). These data are consistent with a dual role for *KNAT2 KNAT6* in AZ initiation (this study) and activation of abscission (Shi et al., 2011). Similar to *KNAT2 KNAT6*, inactivation of *ATH1* partially rescues *bp-2* silique orientation defects and misexpression is observed in *bp-2* pedicels (Khan et al. 2012b). However, a role for *ATH1* in activation of abscission with *KNAT2* and *KNAT6* has not been tested.

To determine the contribution of *ATH1* in the activation of the abscission, *ATH1* expression was first examined in wild type and *bp-2* flowers using a GUS reporter gene (Figure 3.8). In wild type, *ATH1* was strongly expressed in the AZ of flowers between positions 2 to 6. At position 8, expression was diminished in the AZ and absent at positions 10 and 12. As anticipated, *ATH1* expression was prolonged in *bp-2* flower receptacles and pedicels. Expression in the AZ remained strong at position 8 and was maintained in *bp-2* pedicels until position 12. These data indicate that BP restricts *ATH1* expression at the base of flowers, similar to *KNAT2* and *KNAT6*.

Next, I compared flower morphology and abscission phenotypes of *bp-2* and *bp-2 ath1* double mutants (Figure 3.9). Mild sepal fusions were observed in *bp-2* and *bp-2 ath1* flowers similar to *ath1* mutants (see also Figure 3.1). Fruit orientation in *bp-2* mutants was partially corrected in *bp-2 ath1* double mutants as previously reported (Khan et al., 2012a). Quantitative analysis of abscission confirmed that *bp-2* mutants shed their floral organs about one position earlier than wild type (position  $5.7 \pm 0.2$  versus position  $6.4 \pm 0.2$ ). This early abscission was abolished in *bp-2 ath1* double mutants where organs were shed with delayed kinetics (position  $10.9 \pm 0.8$ ) similar to *ath1* (position  $9.0 \pm 0.8$ ). SEM imaging depicted a saddle-shaped AZ for wild type whereas medial enlargement of the AZ in *bp-2* generated a muffin top-like shape (Figure 3.9K; Supplemental Figure S3 and Supplemental Figure S6). AZ morphology in *ath1 bp-2* double mutants was more disrupted compared to either single mutant (compare to Figure 3.4F). Interestingly, this increased disorganization in *ath1 bp-2* mutants did not translate to a significant delay in abscission compared to the *ath1* single mutants. Petal break strength measurements showed a similar patterning of loosening for *ath1* and *bp-2 ath1* mutants (Figure 3.10). These data confirm that AZs do not need to be organized to be functional, shown previously for *bp-3* and *35S:IDA* plants (Shi et al, 2011). Overall, my data indicate that BP spatially and temporally restricts *ATH1* expression in the AZ. My data also show that inactivation of *ATH1* eliminates the premature abscission of *bp-2* mutants but leads to increased proliferation and disorganization of cells in the AZ. Further experiments are required fully determine if *ATH1* promotes abscission by the same mechanism as *KNAT2* and *KNAT6*.

### **3.5 BOP1/2 contribute to activation of abscission**

BP restricts *BOP1/2* expression to boundaries in the inflorescence where *BOP1/2* are positive upstream regulators of *ATH1* and *KNAT6* (Khan et al., 2012b; Hepworth and Pautot, 2015; Khan et al., 2015). Thus, *IDA* signaling to inhibit BP activity is predicted to increase *BOP1/2*

activity in AZs to promote abscission, leading to increased expression of *ATH1/KNAT6* and possibly *KNAT2*. Since *bop1 bop2* mutants do not form AZs, transgenic plants overexpressing *BOP1* (*BOP1-o/e*) were characterized for flower and abscission defects (Figure 3.11). SEM imaging of flowers showed no obvious boundary defects in position 2 flowers (Figure 3.11B). Quantitative analysis of *BOP1 o/e* plants demonstrated acceleration of abscission. Floral organs in the *BOP1 o/e* line abscised about 1.5 positions earlier than wild type (position  $4.9 \pm 0.1$  versus position  $6.4 \pm 0.3$ ). Compatible with these data, *BOP1 o/e* floral receptacles showed rounded AZ cells at position 4 compared to wild type at position 6 (Figure 3.11GH). At positions 6 and higher, fully formed AZs were compact relative to wild-type and a deep groove formed between the receptacle and the base of the fruit. These collective data agree with a role for *BOP1/2* in fruit boundary patterning and activation of abscission, likely upstream of *ATH1/KNAT2/KNAT6*.

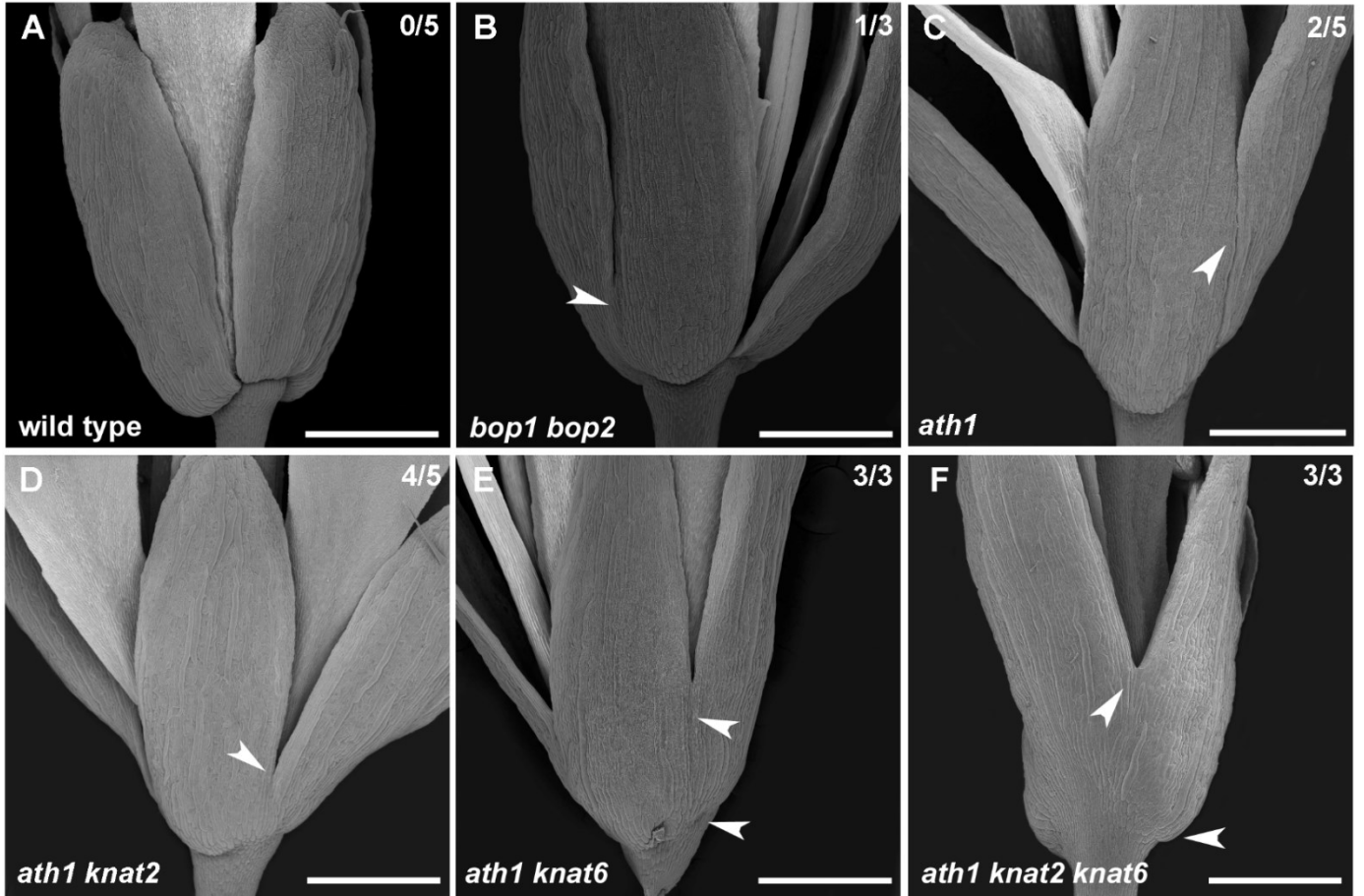


**Figure 3.1 SEM images of wild type and boundary gene mutants.**

Representative images showing position 2 flowers. Numbers at the top right of panels indicate frequency of sepal-fusion defects. A, wild type showing well-separated sepals and distinct boundaries. B, *bop1 bop2* mutant showing occasional mild fusion of sepals (arrow head). C, *ath1* mutant showing occasional fused sepals (arrow head). D, *ath1 knat2* mutant showing moderate fusion of sepals (arrow head). E, *ath1 knat6* mutant showing frequent strong fusion of sepals and smooth boundaries at the base of the flower (arrow heads). F, *ath1 knat2 knat6* mutant showing frequent strong fusion of sepals and smooth boundaries at the base of the flower (arrow heads). Scale bars: 500  $\mu\text{m}$ .

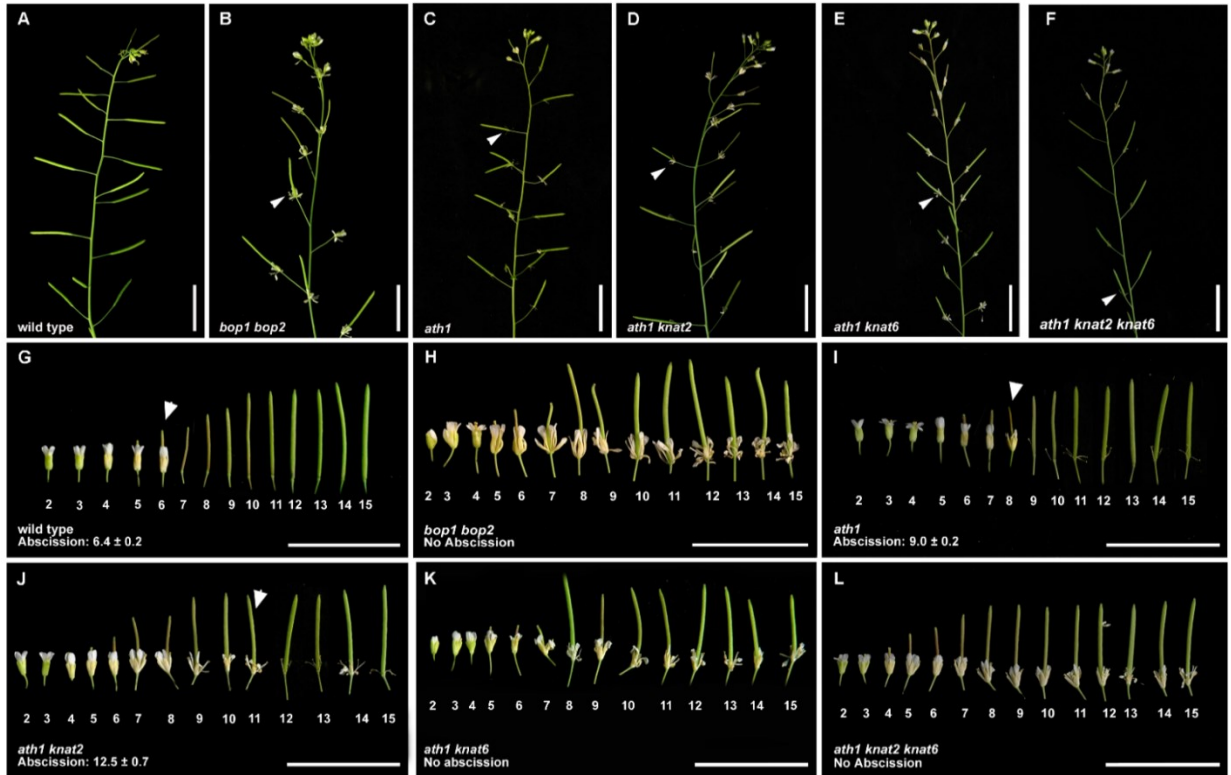


### Figure 3.2 Abscission analysis of wild type and boundary gene mutants.

Representative images are shown. A-F, Inflorescence apices. Wild type *Arabidopsis* plants (Col-0) shed their floral organs while boundary mutants partially or fully retain their floral organs. Arrow heads, floral organs that are retained by mutants with abscission defects. G-L, Abscission series for wild type and mutant flowers/fruits at positions 2-15 on the inflorescence. Arrow heads, initiation of abscission defined as the position at which organs start to detach with gentle mechanical touch. Numerical data (bottom left) indicate mean position for initiation of abscission  $\pm$  standard error (n=20 plants per genotype). G, wild type floral organs abscise between positions 5 and 7. H, *bop1 bop2* floral organs never abscise. I, *ath1* showing a slight delay in abscission compared to wild type; stamens are lightly retained. J, *ath1 knat2* showing delayed abscission compared to *ath1*; organs detach with slight force. K, *ath1 knat6* showing strongly attached floral organs that never abscise. L, *ath1 knat2 knat6* showing strongly attached floral organs that never abscise. Scale bars: 1.5 cm.

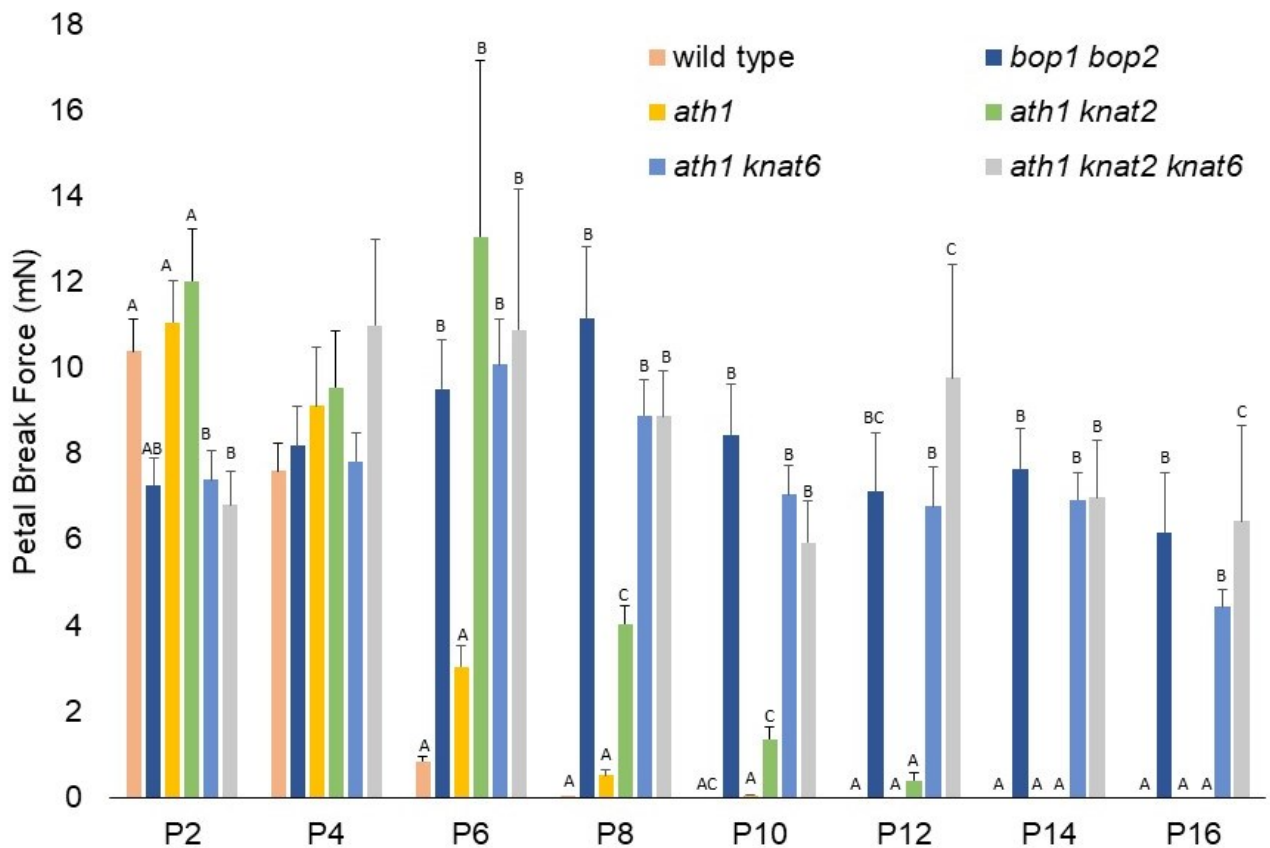


**Figure 3.3 Petal break strength measurements for wild type and boundary mutants.**

The average force required to remove petals from flowers at position 2, 4, 6, 8, 10, 12, 14 and 16 was measured using a petal break strength meter ( $n \geq 20$  petals per node per genotype). The petal break strength of wild type, *ath1*, and *ath1 knat2* flowers decreases with floral position. All other mutants showed little change in force over time. Error bars, standard error of the mean. Uppercase letters represent significant differences between genotypes at each position ( $p \leq 0.05$ , one-way ANOVA with Tukey's post-hoc test).

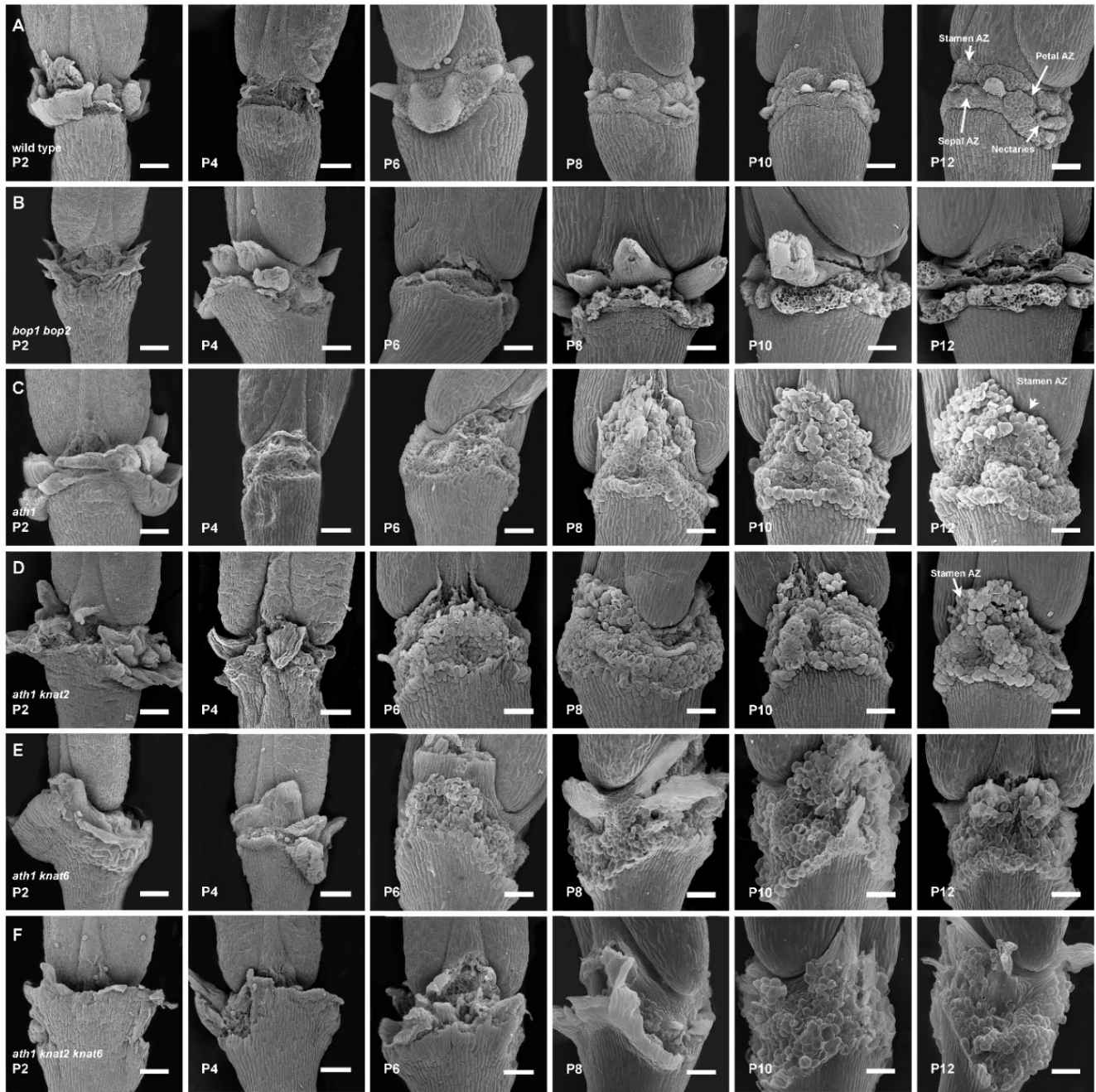


**Figure 3.4 SEM micrographs showing morphology of wild type and boundary mutant receptacles.**

Representative images showing AZs at positions 2, 4, 6, 8, 10, and 12. The fracture plane on the receptacle was observed following removal or natural abscission of floral organs. A, wild type fracture planes showing progression from broken cells (position 2) to rounded cells (position 6) to protective surface cells (position 12). B, *bop1 bop2* fracture planes showing broken cells at all positions. C, *ath1* fracture planes showing partially disorganized cells, particularly in stamen AZs (arrow). D, *ath1 knat2* fracture planes, showing increased disorganization of AZ cells (arrow). E, *ath1 knat6* fracture planes, showing increased disorganization of AZ cells. F, *ath1 knat2 knat6* fracture planes showing broken cells (at position 6) and progressively increased disorganization and enlargement of the AZ. Scale bars: 100µm.

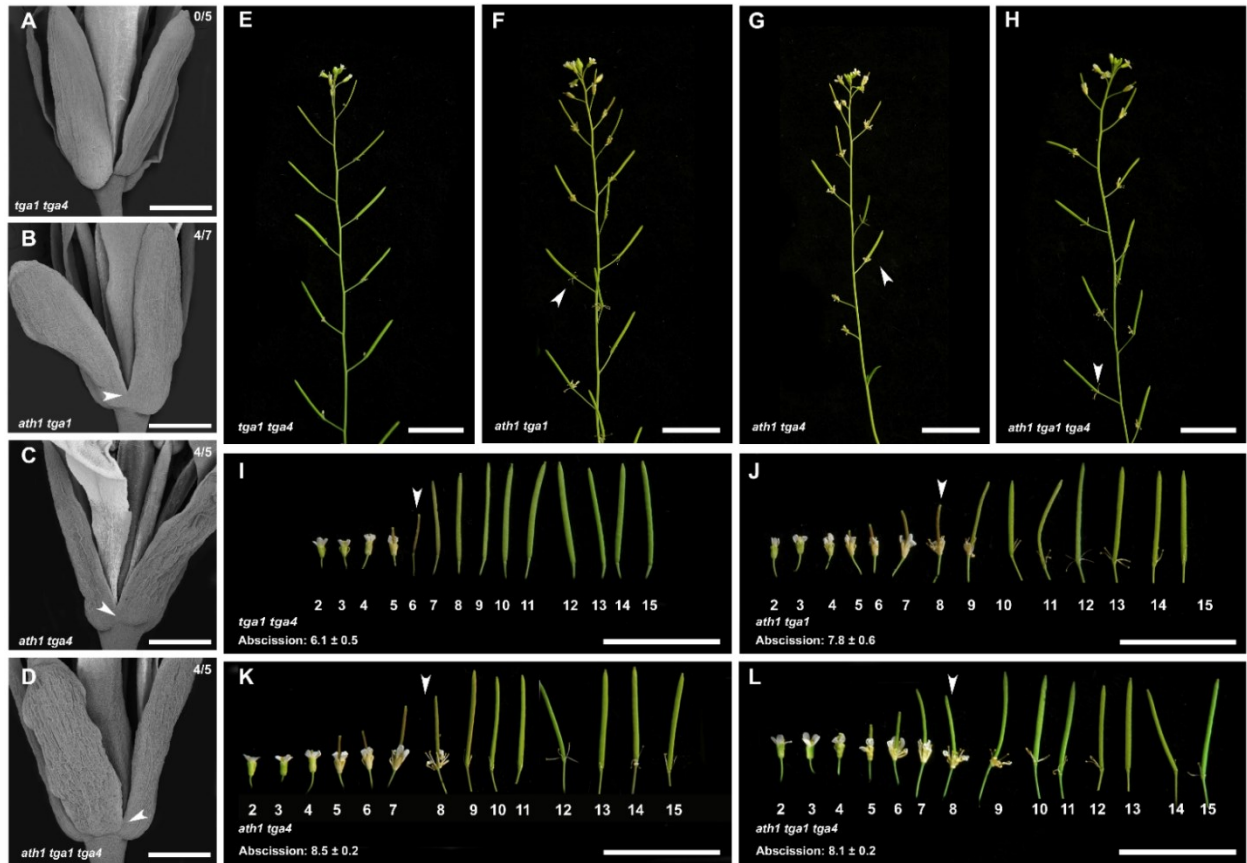


**Figure 3.5 Analysis of floral morphology and abscission in *tga1 tga4*, *ath1 tga1*, *ath1 tga4*, and *ath1 tga1 tga4* mutants.**

Representative images are shown. A-D, SEM images showing *ath1*, *ath1 tga1*, *ath1 tga4*, and *ath1 tga1 tga4* mutant flowers at position 2. Numbers at the top right of panels indicate frequency of sepal-fusion defects (arrows). D, represents a severe fusion phenotype of *ath1 tga4*. E-H, Inflorescence apices showing that *tga1 tga4* mutants shed their floral organs at the same approximate position as wild type whereas abscission in *ath1 tga1*, *ath1 tga4*, and *ath1 tga1 tga4* is slightly delayed, with prolonged attachment of stamens similar to *ath1* mutants (arrow heads). I-L, Abscission series for wild type and mutant flowers/fruit at positions 2-15 on the inflorescence. Arrow heads, initiation of abscission defined as the position at which organs start to detach with gentle mechanical touch. Numerical data (bottom left) indicate mean position for initiation of abscission  $\pm$  standard error (n=20 plants per genotype). I, *tga1 tga4* floral organs abscise between positions 5 and 7, similar to wild type. J, *ath1 tga1* showing slight retention of stamens, similar to *ath1*. K, *ath1 tga4* showing slight retention of stamens, similar to *ath1*. L, *ath1 tga1 tga4* showing slight retention of stamens, similar to *ath1*. Scale bars: A-D, 500  $\mu$ m; E-L, 1.5 cm.

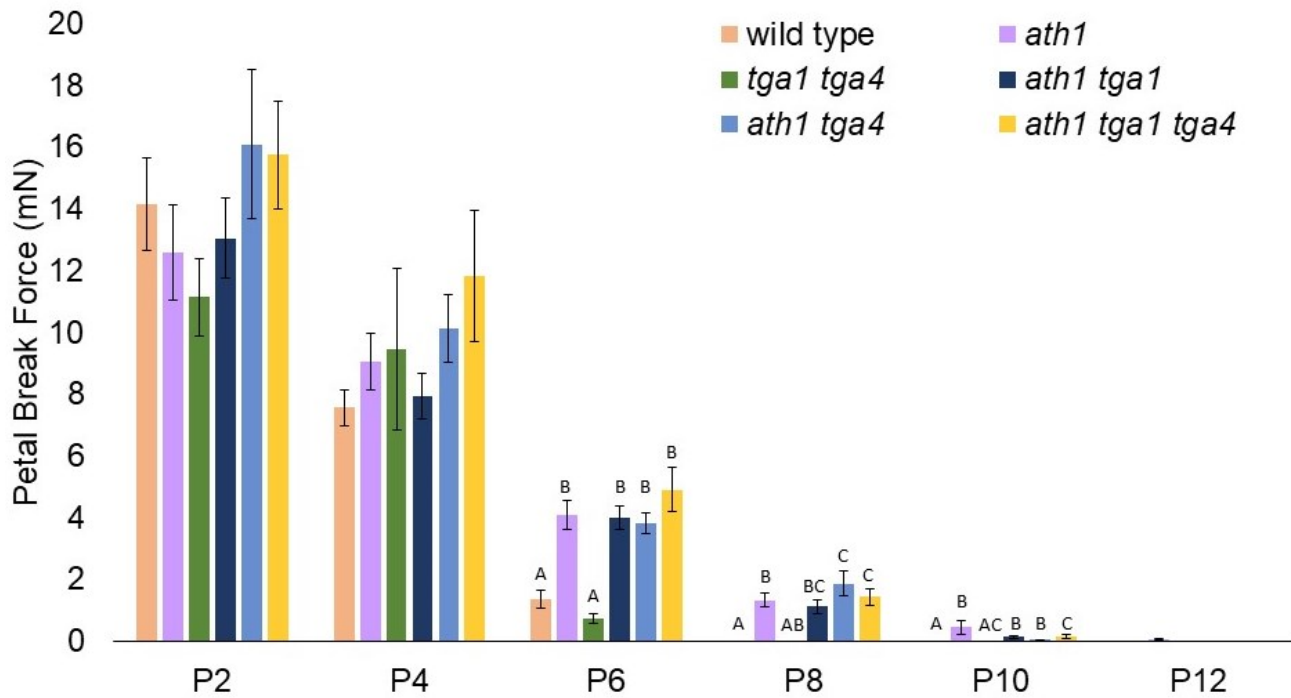


**Figure 3.6** Petal break strength measurements for wild type, *tga1 tga4*, and *ath1*, *ath1 tga1*, *ath1 tga4*, and *ath1 tga1 tga4* mutants.

Data show the average force required to remove petals from flowers at position 2, 4, 6, 8, 10, 12, 14 and 16 ( $n \geq 15$  petals per node per genotype). Petal break strength of wild type and *tga1 tga4* flowers decreases between positions 2 and 6, while all other mutants show a delay in abscission of 4 to 6 positions. Error bars, standard error of the mean. Uppercase letters represent significant differences between genotypes at each position ( $p \leq 0.05$ , one-way ANOVA with Tukey's post-hoc test).

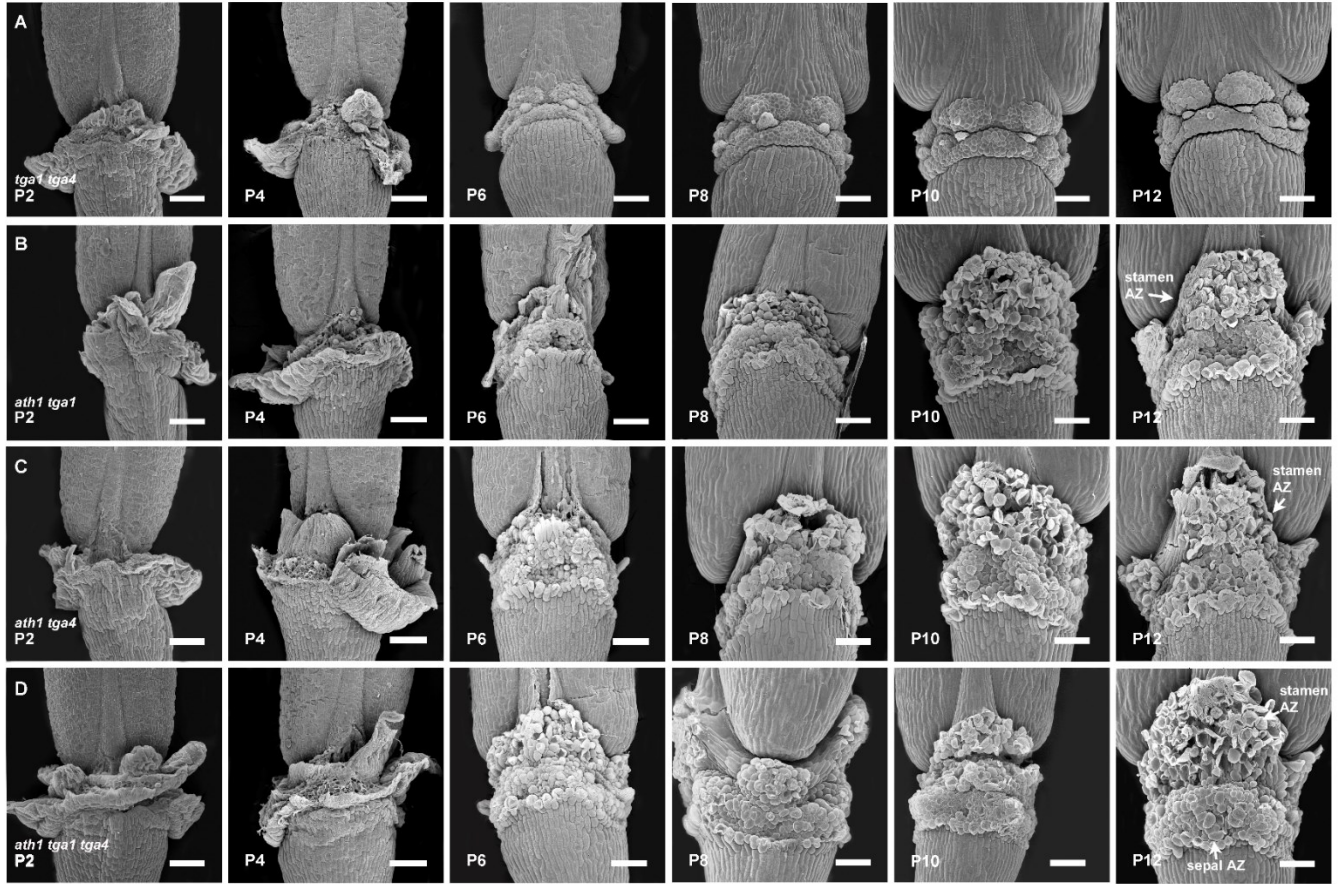


**Figure 3.7 SEM micrographs showing morphology of floral AZs in *tga1 tga4* and *ath1*, *ath1 tga1*, *ath1 tga4*, and *ath1 tga1 tga4* mutants.**

Representative images showing AZs at positions 2, 4, 6, 8, 10, and 12. The fracture plane on the receptacle was observed following removal or natural abscission of floral organs. A, *tga1 tga4* fracture planes are similar to wild type, showing progression from broken cells (position 2) to rounded cells (position 6) to protective surface cells (position 12). B, *ath1 tga1* fracture planes are similar to *ath1*, showing partially disorganized cells, particularly in stamen AZs (arrow). C, *ath1 tga4* fracture planes are similar to *ath1*, showing partially disorganized cells in stamen AZs (arrow). D, *ath1 tga1 tga4* fracture planes, showing disorganization of stamen AZ cells similar to *ath1* plus enlargement of petal and sepal AZs (arrows). Scale bars: 100  $\mu$ m.

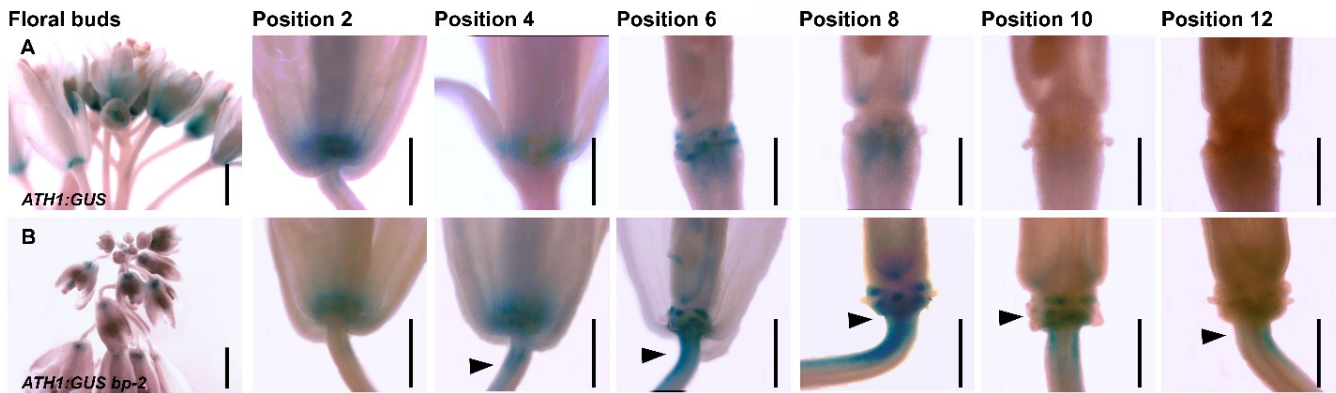


**Figure 3.8** *ATH1:GUS* expression in wild type and *bp-2* mutant flowers.

Representative images of stained tissue showing inflorescence apices and detached flowers/fruits at positions 2, 4, 6, 8, 10, and 12. A, Wild type showing strong AZ expression at positions 2, 4, and 6; weak AZ expression at position 8; little or no AZ expression at positions 10 and 12. B, *bp-2* mutant showing expanded and prolonged expression in the AZ and floral pedicel continuing to position 12 (arrow heads). Scale bars: 0.5 mm, except floral buds = 1 mm.

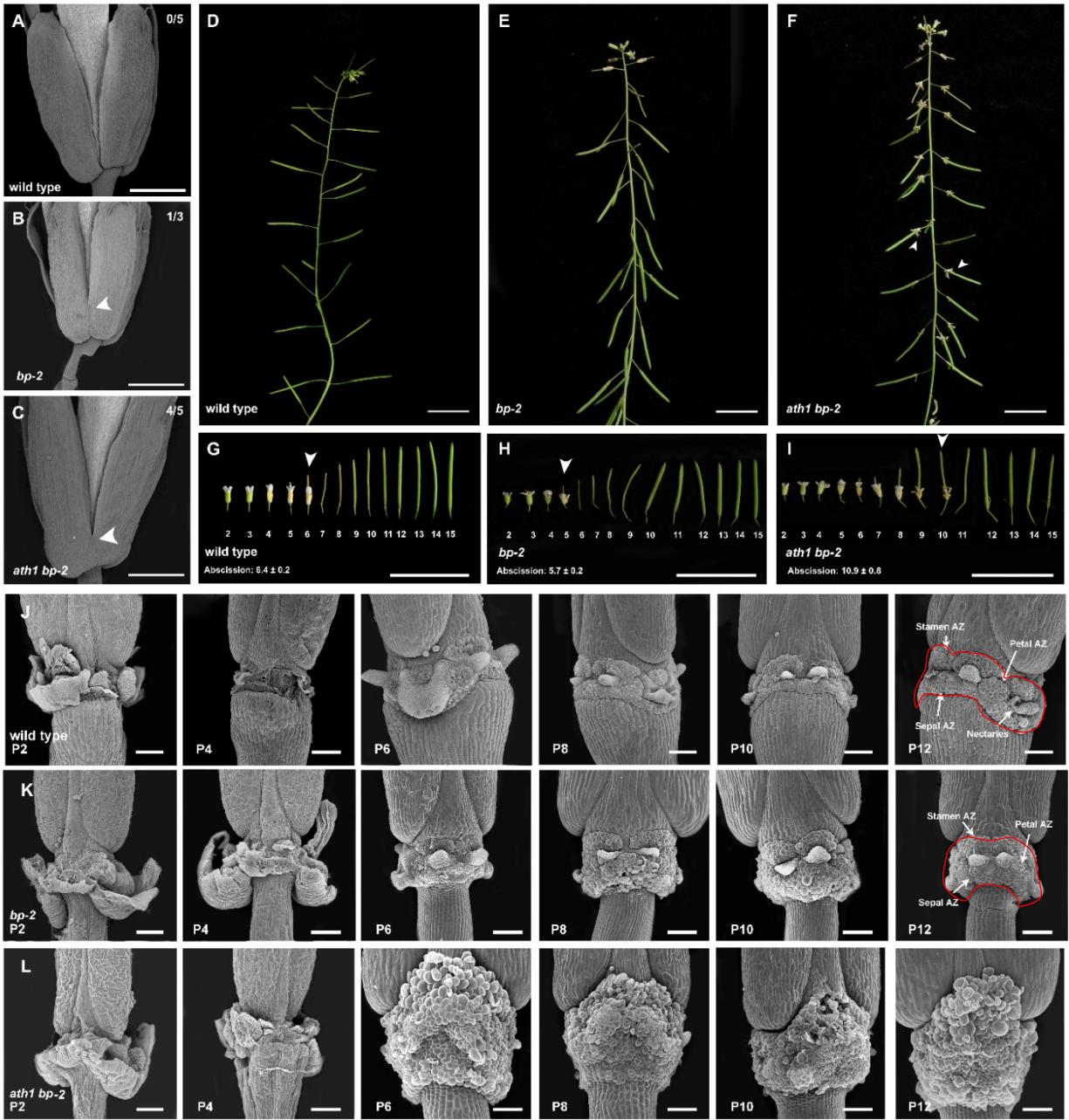


**Figure 3.9 Interaction of *BP* and *ATH1* in abscission.**

A-C, SEM images of wild type, *bp-2*, and *ath1 bp-2* mutants flowers at position 2. Arrow heads indicate fusion of the sepals. D-F, Inflorescence apices for wild type and mutants: *bp-2* and *ath1 bp-2*. Fruit orientation defects in *bp-2* single mutants are partially corrected in *bp-2 ath1* double mutants. Double *bp-2 ath1* mutants flowers partially retain floral organs similar to *ath1* mutants (arrow heads). G-I, Abscission series showing wild type and mutant flowers/fruit at positions 2-15 on the inflorescence. Arrow heads, initiation of abscission defined as the position at which organs start to detach with gentle mechanical touch. Numerical data (bottom left) indicate mean position for initiation of abscission  $\pm$  standard error (n=20 plants per genotype). J-L, SEM micrographs showing wild type and mutant AZs at positions 2, 4, 6, 8, 10, and 12 on the inflorescence. The AZ region in *bp-2* flowers has a different shape (outlined in red) compared to wild type with further disorganized expansion in the *ath1 bp-2* mutant. Scale bars: A-C, 500  $\mu$ m; D-F, 1.5 cm; J-L, 100  $\mu$ m.

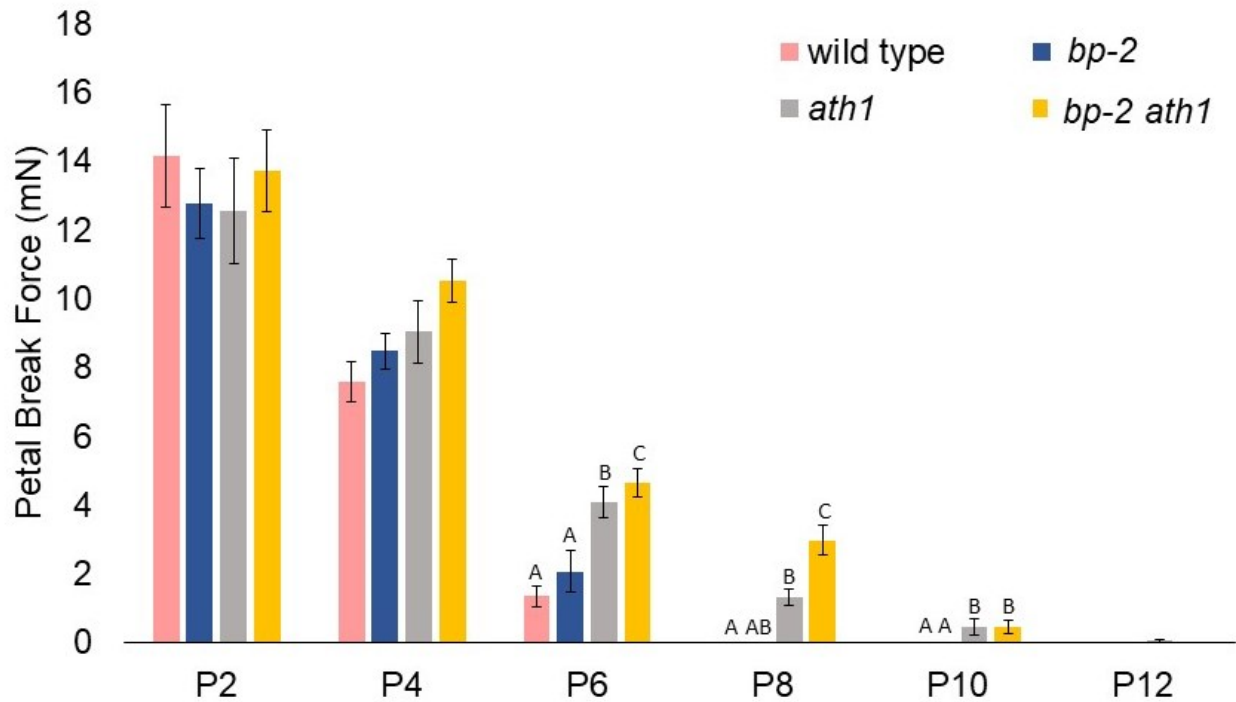


**Figure 3.10 Petal break strength measurements for wild type, *bp-2*, *ath1*, and *bp-2 ath1* mutants.**

Data show the average force required to remove petals from flowers at position 2-16 along the inflorescence ( $n \geq 15$  petals per node per genotype). Petal break strength of wild type and *bp-2* flowers decreases with age between positions 2 and 6 on inflorescence. Abscission is delayed by 2- 4 positions in *ath1* and *ath1 bp-2* mutants. Error bars, standard error of the mean. Uppercase letters represent significant differences between genotypes at each position ( $p \leq 0.05$ , one-way ANOVA with Tukey's post-hoc test).

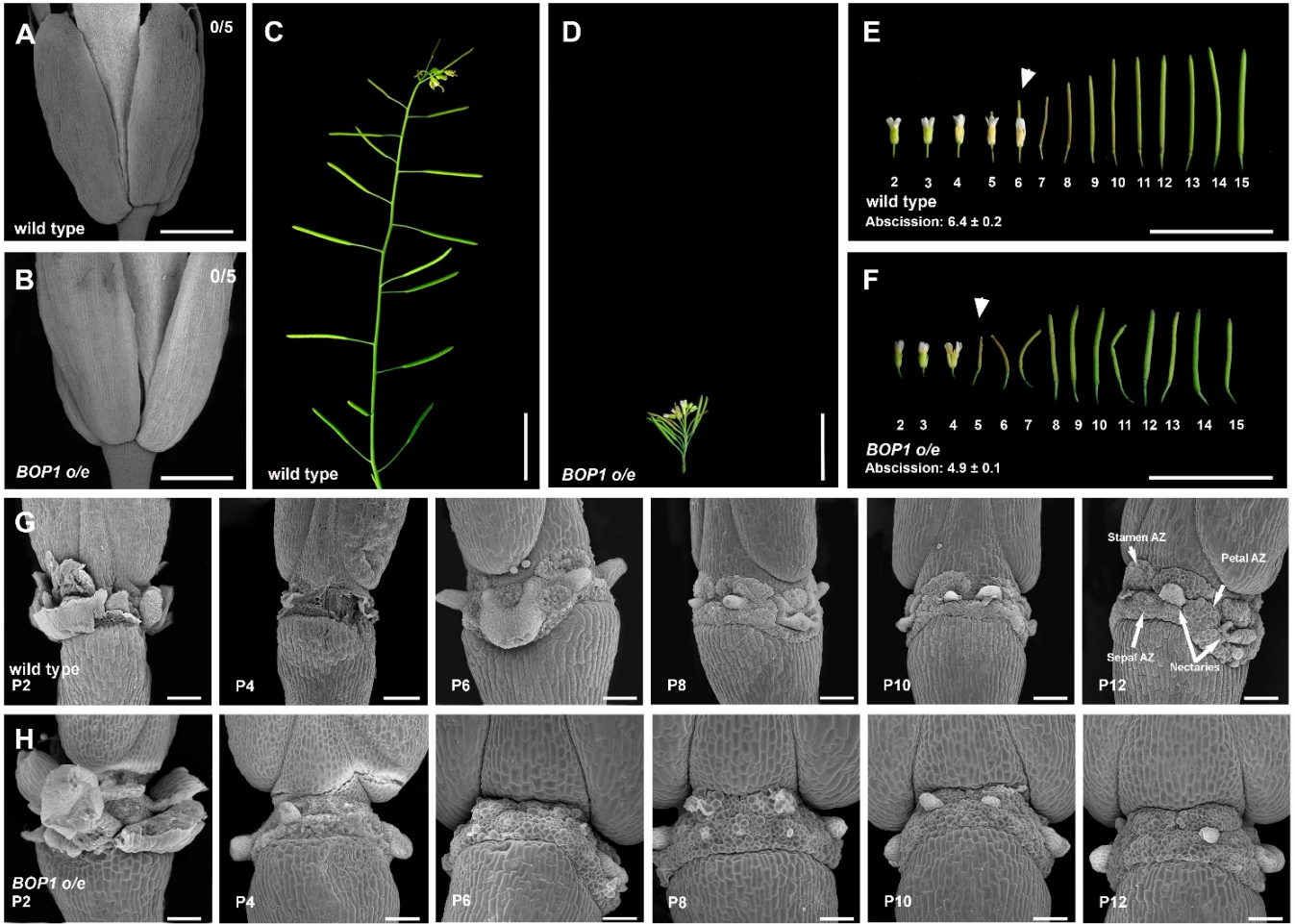


**Figure 3.11 Abscission phenotype of *BOP1* overexpressing transgenic plants.**

A-B, Inflorescence apices of wild type and *BOP1* overexpressing (*BOP1 o/e*) transgenic plants, which exhibit a dwarf phenotype (Norberg et al., 2005). C-D, Abscission series showing wild type and mutant flowers/fruit at positions 2-15 on the inflorescence. Arrow heads, initiation of abscission defined as the position at which organs start to detach with gentle mechanical touch. Numerical data (bottom left) indicate mean position for initiation of abscission  $\pm$  standard error (n=20 plants per genotype). Abscission in *BOP1 o/e* is about one position earlier than wild type. E-F, SEM images of wild type and *BOP1 o/e* mutants flowers at position 2. No organs were fused. G-H, SEM images showing AZ morphology in wild type and mutant flowers/fruit at positions 2, 4, 6, 8, 10, and 12. Fracture planes in *BOP1 o/e* mutant AZs show smoothed cells at position 4 compared to position 6 in wild type. Scale bars: A-D, 1.5 cm; E-F, 500  $\mu$ m; G-H, 100  $\mu$ m.

## CHAPTER 4 : DISCUSSION

Abscission is an essential process that allows plants to discard unwanted organs. Detachment can occur as a natural part of development or as a defense strategy. AZs form at organ boundaries (Hepworth and Pautot, 2015). However, the role of boundary genes in abscission is only partially characterized. *BOP1/2* and three genes of the TALE homeobox family defined by *ATH1/KNAT2/KNAT6* form a conserved module, important for boundary patterning throughout the life cycle (Hepworth and Pautot, 2015). Loss-of-function studies identified *BOP1/2* as essential for AZ formation (McKim et al., 2008). *ATH1* has a specific role in the initiation of stamen AZs (Gómez-Mena and Sablowski, 2008) and *KNAT2* and *KNAT6* are described as having a role in activation of abscission but several evidences suggest a role for *KNAT6* and *KNAT2* (see below) during AZ initiation (Shi et al., 2011). My thesis provides evidence of a role for this boundary module during AZ initiation and separation stages of abscission. Specifically, my data show that: 1) *KNAT6* and *KNAT2* genes contribute to AZ initiation with *ATH1*, 2) these genes restrict the size and control the organization of AZs, and 3) *BOP1/2* and *ATH1* likely contribute to organ separation. Studies using a *BOP1* gain-of-function line suggest a potential role for *BOP1/2* in the activation of abscission. Further experiments are required to determine placement of *ATH1* in the abscission activation pathway.

### 4.1 TALE genes are required for successive steps of abscission

*BOP1/2* are required for AZ formation (McKim et al., 2008). However, the cellular and molecular mechanisms that underlie AZ initiation are largely unknown. My data establish a role for *ATH1/KNAT2/KNAT6* in this process. SEM imaging of flowers revealed that mutations in *BOP1/2* and *ATH1/KNAT2/KNAT6* exhibit boundary-related defects to various degrees, characterized by sepal fusions and smoothening of the constriction that separates sepals from the

floral pedicel. Fusion defects in *bop1 bop2* flowers are relatively mild, with stronger defects in *ath1* single mutants and *knat2 knat6* double mutants and severe defects in *ath1 knat2 knat6* triple mutants. These data indicate overlapping roles for these TALE members in flower boundary formation. Natural detachment of organs is slightly delayed in *ath1* mutants with progressively severe delays in *ath1 knat2*, *ath1 knat6*, and *ath1 knat2 knat6* mutants. In *ath1 knat6* double mutants and *ath1 knat2 knat6* triple mutants, floral organs fail to abscise. Petal break strength measurements showed that loosening of organs is blocked in *ath1 knat2 knat6* triple mutants. In wild type, organs ripped at position 2 but cleanly detached from the AZ at position 4 and onwards with decreasing force indicating progressive weakening of cell adhesion forces. By contrast, broken cells are seen in the fracture plane of *ath1 knat2 knat6* up until position 8 indicating a delay in AZ formation. At later positions, pulled organs detach cleanly from the AZ suggesting a problem in the separation process. Consistent with these data, premature abscission in *IDA* overexpression lines is abolished by mutation of *KNAT2* and *KNAT6* and organs show prolonged attachment (Shi et al., 2011). Future experiments will test if overexpression phenotypes of *IDA* are likewise abolished by mutation of *ATH1*. Plants that overexpress *IDA* show the excess accumulation of arabinogalactans in AZs (Stenvik et al., 2006). Paradoxically, this phenotype is also observed in *ath1*, *ath1 knat2*, *ath1 knat6*, and *ath1 knat2 knat6* mutants (Supplemental Figure S7). Future work will test if separation defects in *ath1 knat2 knat6* triple mutants are linked to flaws in the separation layer and/or lignified layer(s) of the AZ.

*BOP1/2* are expressed in both the separation and lignified layers of the AZ (Supplemental Figure S8). In *bop1 bop2* mutants, ROS are depleted and cells at the base of separating organs fail to lignify (Lee et al., 2018). ROS produced by NADPH oxidases promote the free-radical coupling of lignin monomers (Lee et al., 2018). Lignin serves as a mechanical brace and diffusion barrier

for precise localization of hydrolytic enzyme activity in the AZ. Defects in lignin deposition delay organ separation and impair surface integrity of protective epidermal cells following abscission (Lee et al., 2018). *ATH1* and *KNAT6* but not *KNAT2* are also expressed in the lignified layer (Supplemental Figure S8). All three genes promote stem lignification downstream of *BP/KNAT1* suggesting a similar role in AZs (Khan et al., 2012a; Khan et al., 2012b; Hepworth and Pautot, 2015). To test if *ATH1*, *KNAT2*, and *KNAT6* promote lignification in AZs, loss-of-function mutants will be analyzed for defects in ROS production and lignin deposition through the use of staining techniques.

Progressive loss of boundary TALE activity also impacts the size and organization of the AZ. SEM images of triple mutant *ath1 knat2 knat6* receptacles depict an enlarged and disorganized separation layer. Separation layer cells newly exposed on the fruit receptacle normally adopt epidermal fate and secrete a protective layer of cuticle following abscission (Lee et al., 2018). Deposition of this secreted layer relies heavily on membrane vesicle trafficking. Mutations in the ARF-GAP gene *NEVERSHED* disrupt vesicle transport. Loss-of-function *nev* mutants never shed their floral organs and also exhibit enlarged and disordered AZs when organs are forcibly detached (Liljegren et al., 2009; Liu et al., 2013). The *nev* phenotype is similar to *ath1 knat2 knat6* triple mutants suggesting a possible link. Primers for measuring *IDA*, *HAE*, and *NEV* transcript level in wild type and boundary mutant AZs have been validated and will be used to probe for possible changes in gene expression (Supplemental Table S2). It may also be worth testing if *ath1 knat2 knat6* mutants have vesicle trafficking defects similar to *nev* mutants.

#### **4.2 Clade I TGAs play a minor role in the sizing of the AZ**

Clade I TGA bZIPs are expressed in inflorescence boundaries where they interact with BOP1/2 for activation of *ATH1* (Wang et al., 2018). Consistent with functions for these genes in

the same pathway, inactivation of *TGA1* and *TGA4* did not worsen delayed abscission in *ath1* mutants. However, SEM imaging showed that sepal AZs in *ath1 tga1 tga4* receptacles were significantly enlarged and disorganized compared to *ath1* single mutants. These data suggest a minor role for TGA1/4 in controlling AZ morphology. These data suggest that other TGA transcription factor or other classes of transcription factors are involved.

### 4.3 Interaction with IDA pathway

The abscission signaling peptide IDA has been conserved during the evolution of flowering plants (Butenko et al., 2003; Estornell et al., 2015; Stø et al., 2015; Tranbarger et al., 2017). In Arabidopsis, IDA signaling inhibits BP/KNAT1 activity thereby releasing brakes on *KNAT2* and *KNAT6*, whose activities promote separation (Shi et al., 2011). Similar to *KNAT2* and *KNAT6*, BP spatially and temporally restricts *ATH1* expression in the AZ and inactivation of *ATH1* reverses the premature abscission of *bp* mutants. However, greater disorganization of *bp ath1* AZ cells contrasts with *bp-3 knat2 knat6* mutants where AZ morphology is normalized (Shi et al., 2011). A precise role for *ATH1* in organ separation can be tested by examining *35S:ATH1* plants for premature abscission and by examining if mutation of *ATH1* suppresses overexpression phenotypes of *35S:IDA* plants.

It is tempting to speculate that an increase in IDA signaling and decrease in BP/KNAT1 activity promotes *BOP1/2* activity, thereby maintaining appropriate levels of *ATH1/KNAT2/KNAT6* gene expression in the AZ. Transgenic plants that overexpress *BOPI* abscise their organs about one position earlier than wild type showing a positive role. Future experiments will test if early abscission in *bp* mutants correlates with higher levels of *BOPI* or *BOP2* expression in AZs. Antagonistic interactions between BP and boundary genes are observed in the inflorescence, where *BOPI/2* and *ATH1/KNAT2/KNAT6* function antagonistically

downstream of *BP* to control the timing of lignin deposition during stem maturation (Ragni et al., 2008; Khan et al., 2012a; Khan et al., 2012b).

#### **4.4 Links between innate immunity and abscission**

In summary, *ATH1/KNAT2/KNAT6* contributes to two steps in the abscission process: AZ initiation and organ separation. Discovering the transcriptional targets of boundary genes during abscission is an important next step. Recent work in our lab has uncovered a role for BOP1/2 in innate immunity, which has intriguing conceptual overlaps with abscission. Abscission and innate immunity signaling pathways involve similar membrane receptors, signal transduction machinery, and downstream activation of enzymes that modify and reinforce the cell wall (Meir et al., 2011; Patharkar and Walker, 2017). Transcriptome work in our lab shows that BOP1/2 promote the expression of numerous innate immunity genes (Chris Bergin, M.Sc. thesis) including NADPH oxidases and peroxidases important for lignin deposition in the abscission zone (Lee et al., 2018). Future work will examine functional overlaps between boundary genes in abscission and innate immunity.

#### **4.5 Concluding remarks**

In closing, boundary genes represent promising molecular targets for engineering abscission-resistant crops. Manipulation of boundary genes or their targets has the potential to impact crucial steps in the abscission pathway by altering AZ structure and biochemistry. Furthermore, this knowledge relates to abscission-related traits like pod shatter. Pod dehiscence for seed dispersal involves the development of abscission zones along boundaries in the fruit called valve margins. Dehiscence zones in an *Arabidopsis* fruit are composed of adjacent lignified and separation layers nearly identical to those in abscission zones of the flower. Thus, abscission and

dehiscence are related mechanisms (Dong and Wang, 2015). Future work will compare the role of boundary genes in abscission and pod shatter for applications in crops.

## REFERENCES

- Adamczyk BJ, Lehti-Shiu MD, Fernandez DE** (2007) The MADS domain factors AGL15 and AGL18 act redundantly as repressors of the floral transition in Arabidopsis. *Plant J* **50**: 1007-1019
- Anthony MF, Coggins JCW** (1999) The efficacy of five forms of 2,4-D in controlling preharvest fruit drop in citrus. *Sci Hortic* **81**: 267-277
- Belles-Boix E, Hamant O, Witiak SM, Morin H, Traas J, Pautot V** (2006) *KNAT6*: an Arabidopsis homeobox gene involved in meristem activity and organ separation. *Plant Cell* **18**: 1900-1907
- Bleeker AB, Patterson SE** (1997) Last exit: senescence, abscission, and meristem arrest in Arabidopsis. *Plant Cell* **9**: 1169-1179
- Bürglin TR** (1997) Analysis of the TALE superclass homeobox genes (MEIS, PBC, KNOX, Iroquois, TGIF) reveals a novel domain conserved between plants and animals. *Nucleic Acids Res* **25**: 4173-4180
- Burr CA, Leslie ME, Orlowski SK, Chen I, Wright CE, Daniels MJ, Liljegren SJ** (2011) CAST AWAY, a membrane-associated receptor-like kinase, inhibits organ abscission in Arabidopsis. *Plant Physiol* **156**: 1837-1850
- Butenko MA, Patterson SE, Grini PE, Stenvik G-E, Amundsen SS, Mandal A, Aalen RB** (2003) *INFLORESCENCE DEFICIENT IN ABSCISSION* controls floral organ abscission in Arabidopsis and identifies a family of putative ligands in plants. *Plant Cell* **15**: 2296-2307
- Celton J-M, Kelner J-H, Martinez S, Bechti A, Touhami AK, James MJ, Durel C-E, Laurens F, Costes E** (2014) Fruit self-thinning: a trait to consider for genetic improvement of apple tree. *PLoS One* **9**: e91016

- Chahtane H, Zhang B, Norberg M, LeMasson M, Thévenon E, Bakó L, Benlloch R, Holmlund M, Parcy F, Nilsson O, Vachon G** (2018) LEAFY activity is post-transcriptionally regulated by BLADE ON PETIOLE2 and CULLIN3 in Arabidopsis. *New Phytologist* (in press)
- Chen M-K, Hsu W-H, Lee P-F, Thiruvengadam M, Chen H, Yang C-H** (2011) The MADS box gene, *FOREVER YOUNG FLOWER*, acts as a repressor controlling floral organ senescence and abscission in Arabidopsis. *Plant J* **68**: 168-185
- Cho SK, Larue CT, Chavalier D, Wang H-Y, Jinn T-L, Zhang S, Walker JC** (2008) Regulation of floral organ abscission in *Arabidopsis thaliana*. *Proc Natl Acad Sci USA* **105**: 15629-15634
- Couzigou JM, Magne K, Mondy S, Cosson V, Clements J, Ratet P** (2016) The legume NOOT-BOP-COCH-LIKE genes are conserved regulators of abscission, a major agronomical trait in cultivated crops. *New Phytol* **209**: 228-240
- Craker LE, Abeles FB** (1969) Abscission: quantitative measurement with a recording abscissor. *Plant Physiol* **44**: 1139-1143
- Dockx J, Quaedvlieg N, Keultjes G, Kock P, Weisbeek P, Smeekens S** (1995) The homeobox gene *ATK1* of *Arabidopsis thaliana* is expressed in the shoot apex of the seedling and in flowers and inflorescence stems of mature plants. *Plant Mol Biol* **28**: 723-737
- Dong Y, Wang Y-Z** (2015) Seed shattering: from models to crops. *Front Plant Sci* **6**: 476
- Edwards K, Johnstone C, Thompson C** (1991) A simple and rapid method for the preparation of plant genomic DNA for PCR analysis. *Nucleic Acid Res* **19**: 1349
- Estornell LH, Augustí J, Merelo P, Talón M, Tadeo FR** (2013) Elucidating mechanisms underlying organ abscission. *Plant Sci* **199-200**: 48-60

- Estornell LH, Wildhagen M, Pérez-Amador MA, Talón M, Tadeo FR, Butenko MA (2015)**  
The IDA peptide controls abscission in Arabidopsis and Citrus. *Front Plant Sci* **6**: 1003
- Faeth SH, Connor EF, Simberloff D (1981)** Early leaf abscission: a neglected source of mortality for folivores. *Am Natl* **117**: 409-415
- Fernandez DE, Heck GR, Perry SE, Patterson SE, Bleeker AB, Fang S-C (2000)** The embryo MADS domain factor AGL15 acts postembryonically: inhibition of perianth senescence and abscission via constitutive expression. *Plant Cell* **12**: 183-197
- Gatz C (2013)** From pioneers to team players: TGA transcription factors provide a molecular link between different stress pathways. *Mol Plant Microb Interact* **26**: 151-159
- Gómez-Gómez L, Boller T (2000)** FLS2: An LRR receptor-like kinase involved in the perception of the bacterial elicitor flagellin in Arabidopsis. *Mol Cell* **5**: 1003-1011
- Gómez-Mena C, Sablowski R (2008)** *ARABIDOPSIS THALIANA HOMEBOX GENE1* establishes the basal boundaries of shoot organs and controls stem growth. *Plant Cell* **20**: 2059-2072
- Hamant O, Pautot V (2010)** Plant development: a TALE story. *CR Biol* **333**: 371-381
- Haughn GW, Somerville C (1986)** Sulfonylurea-resistant mutants of *Arabidopsis thaliana*. *Mol Gen Genet* **204**: 430-434
- He Z, Wang Z-Y, Li J, Zhu Q, Lamb C, Ronald P, Chory J (2000)** Perception of brassinosteroids by the extracellular domain of the receptor kinase BRI1. *Science* **288**: 2360-2363
- Hepworth SR, Pautot V (2015)** Beyond the divide: boundaries for patterning and stem cell regulation in plants. *Front Plant Sci* **6**: 1052

- Hepworth SR, Zhang Y, McKim S, Li X, Haughn GW (2005)** BLADE-ON-PETIOLE-dependent signaling controls leaf and floral patterning in Arabidopsis. *Plant Cell* **17**: 1434-1448
- Jinn T-L, Stone JM, Walker JC (2000)** HAESA, an Arabidopsis leucine-rich repeat receptor kinase, controls floral organ abscission. *Genes Dev* **14**: 108-117
- Kesarwani M, Yoo J, Dong X (2007)** Genetic interactions of TGA transcription factors in the regulation of pathogenesis-related genes and disease resistance in Arabidopsis. *Plant Physiol* **144**: 336-346
- Khan M, Ragni L, Tabb P, Salasini BC, Chatfield S, Datla R, Lock J, Kuai X, Després C, Proveniers M, Yongguo C, Xiang D, Morin H, Citerne S, Hepworth SR, Pautot V (2015)** Repression of lateral organ boundary genes by PENNYWISE and POUND-FOOLISH is essential for meristem maintenance and flowering in *Arabidopsis thaliana*. *Plant Physiol* **169**: 2166-2186
- Khan M, Tabb P, Hepworth SR (2012a)** BLADE-ON-PETIOLE1 and 2 regulate Arabidopsis inflorescence architecture in conjunction with homeobox genes *KNAT6* and *ATH1*. *Plant Signal Behav* **7**: 788-792
- Khan M, Xu H, Hepworth SR (2014)** BLADE-ON-PETIOLE genes: setting boundaries in development and defense. *Plant Sci* **215-216**: 157-171
- Khan M, Xu M, Murmu J, Tabb P, Liu Y, Storey K, McKim SM, Douglas CJ, Hepworth SR (2012b)** Antagonistic interaction of BLADE-ON-PETIOLE1 and 2 with BREVIPEDICELLUS and PENNYWISE regulates Arabidopsis inflorescence architecture. *Plant Physiol* **158**: 946-960

- Kim J** (2014) Four shades of detachment: regulation of floral organ abscission. *Plant Signal Behav* **9**: e976154
- Koornneef M, Meinke D** (2010) The development of Arabidopsis as a model plant. *Plant J* **61**: 909-921
- Lavagi I, Estelle M, Weckwerth W, Beynon J, Bastow R** (2012) From bench to bountiful harvest: A road map for the next decade of Arabidopsis research. *Plant Cell* **24**: 2240-2247
- Lease KA, Cho SK, Walker JC** (2006) A petal break strength meter for Arabidopsis abscission studies. *Plant Methods* **2**: 2
- Lee Y, Yoon TH, Lee J, Jeon SY, Lee JH, Lee MK, Chen H, Yun J, Oh SY, Wen X, Cho HK, Mang H, Kwak JM** (2018) A lignin molecular brace controls precision processing of cell walls critical for surface integrity in Arabidopsis. *Cell* **173**: 1468-1480
- Leslie ME, Lewis MW, Youn J-Y, Daniels MJ, Liljegren SJ** (2010) The EVERSLED receptor-like kinase modulates floral organ shedding in Arabidopsis. *Development* **137**: 467-476
- Lewis MW, Leslie ME, Fulcher EH, Darnielle L, Healy PN, Youn J-Y, Liljegren SJ** (2010) The SERK1 receptor-like kinase regulates organ separation in Arabidopsis flowers. *Plant J* **62**: 817-828
- Li Y, Pi L, Huang H, Xu L** (2012) ATH1 and KNAT2 proteins act together in regulation of plant inflorescence architecture. *J Exp Bot* **63**: 1423-1433
- Liljegren SJ, Leslie ME, Darnielle L, Lewis MW, Taylor SM, Luo R, Geldner N, Chory J, Randazzo PA, Yanofsky MF, Ecker JR** (2009) Regulation of membrane trafficking and organ separation by the NEVERSHED ARF-GAP protein. *Development* **136**: 1909-1918
- Liu B, Butenko MA, Shi C-L, Bolivar-Medina JL, Winge P, Stenvik G-E, Vie AK, Leslie ME, Brembu T, Kristiansen W, Bones AM, Patterson SE, Liljegren SJ, Aalen RB** (2013)

- NEVERSHED* and *INFLORESCENCE DEFICIENT IN ABSCISSION* are differentially required for cell expansion and cell separation during floral organ abscission in *Arabidopsis thaliana*. *J Exp Bot* **17**: 5345-5357
- Mao L, Begum D, Chuang HW, Budiman MA, Szymkowiak EJ, Irish EE, Wing RA** (2000) *JOINTLESS* is a MADS-box gene controlling tomato flower abscission zone development. *Nature* **406**: 910-913
- McKim SM, Stenvik GE, Butenko MA, Kristiansen W, Cho SK, Hepworth SR, Aalen RB, Haughn GW** (2008) The *BLADE-ON-PETIOLE* genes are essential for abscission zone formation in *Arabidopsis*. *Development* **135**: 1537-1546
- Meir S, Philosoph-Hadas S, Sundaresan S, Selvaraj KSV, Burd S, Ophir R, Kochanek B, Reid MS, Jiang C-Z, Lers A** (2011) Identification of defense-related genes newly associated with tomato flower abscission. *Plant Signal Behav* **6**: 590-593
- Meir S, Sundaresan S, Riov J, Agarwal I, Philosoph-Hadas S** (2015) Role of auxin depletion in abscission control. *Stewart Postharvest Review* **2**: 2
- Meng X, Zhou J, Tang J, Li B, de Oliveria MVV, Chai J, He P, Shan L** (2016) Ligand-induced receptor-like kinase complex regulates floral organ abscission in *Arabidopsis*. *Cell Rep* **14**: 1330-1338
- Modrusan Z, Reiser L, K.A. F, Fischer RL, Haughn GW** (1994) Homeotic transformation of ovules into carpel-like structures in *Arabidopsis*. *Plant Cell* **6**: 333-349
- Nam KH, Li J** (2002) BRI1/BAK1, a receptor kinase pair mediating brassinosteroid signaling. *Cell* **110**: 203-212
- Ng M, Yanofsky M** (2001) Function and evolution of the plant MADS-box gene family. *Nat Genet* **2**: 186-195

- Norberg M, Holmlund M, Nilsson O** (2005) The *BLADE ON PETIOLE* genes act redundantly to control the growth and development of lateral organs. *Development* **132**: 2203-2213
- Pandey RK, Herrera WAT, Willegas AN, Pendleton JW** (1984) Drought response of grain legumes under irrigation gradient: III. plant growth. *Agron J* **76**: 557-560
- Patharkar OR, Walker JC** (2015) Floral organ abscission is regulated by a positive feedback loop. *Proc Natl Acad Sci USA* **112**: 2906-2911
- Patharkar OR, Walker JC** (2017) Advances in abscission signaling. *J Exp Bot* **12**: 733-740
- Patterson SE** (2001) Cutting loose. Abscission and dehiscence in Arabidopsis. *Plant Physiol* **126**: 494-500
- Patterson SE, Bolivar-Medina JL, Falbel Tg, Hedtcke JL, Nevarez-McBride D, Maule AF, Zalapa JE** (2016) Are we on the right track: can our understanding of abscission in model systems promote or derail making improvements in less studied crops? *Front Plant Sci* **6**: 1268
- Proveniers M, Rutjens B, Brand M, Smeekens S** (2007) The Arabidopsis TALE homeobox gene *ATH1* controls floral competency through positive regulation of *FLC*. *Plant J* **52**: 899-913
- Ragni L, Belles-Boix E, Gunl M, Pautot V** (2008) Interaction of KNAT6 and KNAT2 with BREVIPEDICELLUS and PENNYWISE in Arabidopsis inflorescences. *Plant Cell* **20**: 888-900
- Roberts JA, Elliott KA, Gonzalez-Carranza ZH** (2002) Abscission, dehiscence, and other cell separation processes. *Annu Rev Plant Biol* **53**: 131-158
- Roberts JA, Whitelaw CA, Gonzalez-Carranza ZH, McManus MT** (2000) Cell separation processes in plants--models, mechanisms, and manipulation. *Annals Bot* **86**: 223-235

- Rutjens B, Bao D, van Eck-Stouten E, Brand M, Smeekens S, Proveniers M** (2009) Shoot apical meristem function in Arabidopsis requires the combined activities of three BEL1-like homeodomain proteins. *Plant J* **58**: 641-654
- Santiago J, Brandt B, Wildhagen M, Hohmann U, Hothorn LA, Butenko MA, Hothorn M** (2016) Mechanistic insight into a peptide hormone signaling complex mediating floral organ abscission. *eLife* **5**: e15075
- Schardon K, Hohl M, Graff L, Pfannstiel J, Schulze W, Stintzi A, Schaller A** (2016) Precursor processing for plant peptide hormone maturation by subtilisin-like serine proteinases. *Science* **354**: 1594-1597
- Sexton R, Roberts JA** (1982) Cell biology of abscission. *Ann Rev Plant Physiol* **33**: 133-162
- Shi CL, Stenvik GE, Vie AK, Bones AM, Pautot V, Proveniers M, Aalen RB, Butenko MA** (2011) Arabidopsis class I KNOTTED-like homeobox proteins act downstream in the IDA-HAE/HSL2 floral abscission signaling pathway. *Plant Cell* **23**: 2553-2567
- Somerville C, Koornneef M** (2002) A fortunate choice: the history of Arabidopsis as a model plant. *Nat Rev Genet* **3**: 883-889
- Stenvik G-E, Butenko MA, Urbanowicz BR, Rose JKC, Aalen RB** (2006) Overexpression of *INFLORESCENCE DEFICIENT IN ABSCISSION* activates cell separation in vestigial abscission zones in Arabidopsis. *Plant Cell* **18**: 1467-1476
- Stenvik G-E, Tandstand NM, Guo Y, Shi C-L, Kristiansen W, Holmgren A, Clark SE, Aalen RB, Butenko MA** (2008) The EPIP peptide of *INFLORESCENCE DEFICIENT IN ABSCISSION* is sufficient to induce abscission in Arabidopsis through the receptor-like kinases HAESA and HAESA-LIKE2. *Plant Cell* **20**: 1805-1817

- Stø ID, Orr RJS, Fooyontphanich K, Jin X, Knutsen JMB, Fischer U, Tranbarger TJ, Nordal I, Aalen RB** (2015) Conservation of the abscission signaling peptide IDA during Angiosperm evolution: withstanding genome duplications and gain and loss of the receptors HAE/HSL2. *Front Plant Sci* **6**: 931
- Taylor JE, Whitelaw CA** (2001) Signals in abscission. *New Phytol* **151**: 323-339
- Tranbarger TJ, Tucker ML, Roberts JA, Meir S** (2017) Editorial: Plant organ abscission: From models to crops. *Front Plant Sci* **8**: 196
- Tucker ML, Kim J** (2015) Abscission research: what we know and what we still need to study. *Stewart Postharvest Review* **2**: 1
- van Doorn WG, Stead AD** (1997) Abscission of flowers and floral parts. *J Exp Bot* **48**: 821-837
- Venglat SP, Dumonceaux T, Rozwadowski K, Parnell L, Babic V, Keller W, Martienssen R, Selvaraj G, Datla R** (2002) The homeobox gene *BREVIPEDICELLUS* is a key regulator of inflorescence architecture in *Arabidopsis*. *Proc Natl Acad Sci USA* **99**: 4730-4735
- Wang Y, Salasini BC, Khan M, Devi B, Bush M, Subramaniam R, Hepworth SR** (2018) Clade I TGA bZIP factors mediate *BLADE-ON-PETIOLE* dependent regulation of *Arabidopsis* development. *Plant Physiol*: (accepted, with revisions)
- Woerlen N, Allam G, Popescu A, Corrigan L, Pautot V, Hepworth SR** (2017) Repression of *BLADE-ON-PETIOLE* genes by KNOX homeodomain protein *BREVIPEDICELLUS* is essential for differentiation of secondary xylem in *Arabidopsis* root. *Planta* **245**: 1079-1090
- Wu X-M, Yu Y, Han L-B, Li C-L, Wang H-Y, Zhong N-Q, Xia G-X** (2012) The tobacco *BLADE-ON-PETIOLE2* gene mediates differentiation of the corolla abscission zone by controlling longitudinal cell expansion. *Plant Physiol* **159**: 835-850

- Xu C, Park SJ, Van Eck J, Lippman ZB** (2016) Control of inflorescence architecture in tomato by BTB/POZ transcriptional regulators. *Genes Dev* **30**: 2048-2061
- Xu M, Hu T, McKim SM, Murmu J, Haughn GW, Hepworth SR** (2010) Arabidopsis BLADE-ON-PETIOLE1 and 2 promote floral meristem fate and determinacy in a previously undefined pathway targeting APETALA1 and AGAMOUS-LIKE24. *Plant J* **63**: 974-989
- Yuan R, Carbaugh DH** (2007) Effects of NAA, AVG, and 1-MCP on ethylene biosynthesis, preharvest fruit drop, fruit maturity, and quality of 'golden supreme' and 'golden delicious' apples. *HortScience* **42**: 101-105
- Zahara MD, Scheurerman RW** (1988) Hand-harvesting jointless vs. jointed-stem tomatoes. *California Agriculture* **42**: 14
- Zhang B, Holmlund M, Lorrain S, Norberg M, Bakó L, Fankhauser C, Nilsson O** (2017) BLADE-ON-PETIOLE proteins act in an E3 ubiquitin ligase complex to regulate PHYTOCHROME INTERACTING FACTOR 4 abundance. *eLife* **6**: e26759
- Zhao M, Yang S, Chen C-Y, Li C, Shan W, Lu W, Cui Y, Liu X, K W** (2015) Arabidopsis BREVIPEDICELLUS interacts with the SWI2/SNF2 chromatin remodeling ATPase BRAHMA to regulate KNAT2 and KNAT6 expression in control of inflorescence architecture. *PLoS Genet* **11**: e1005125

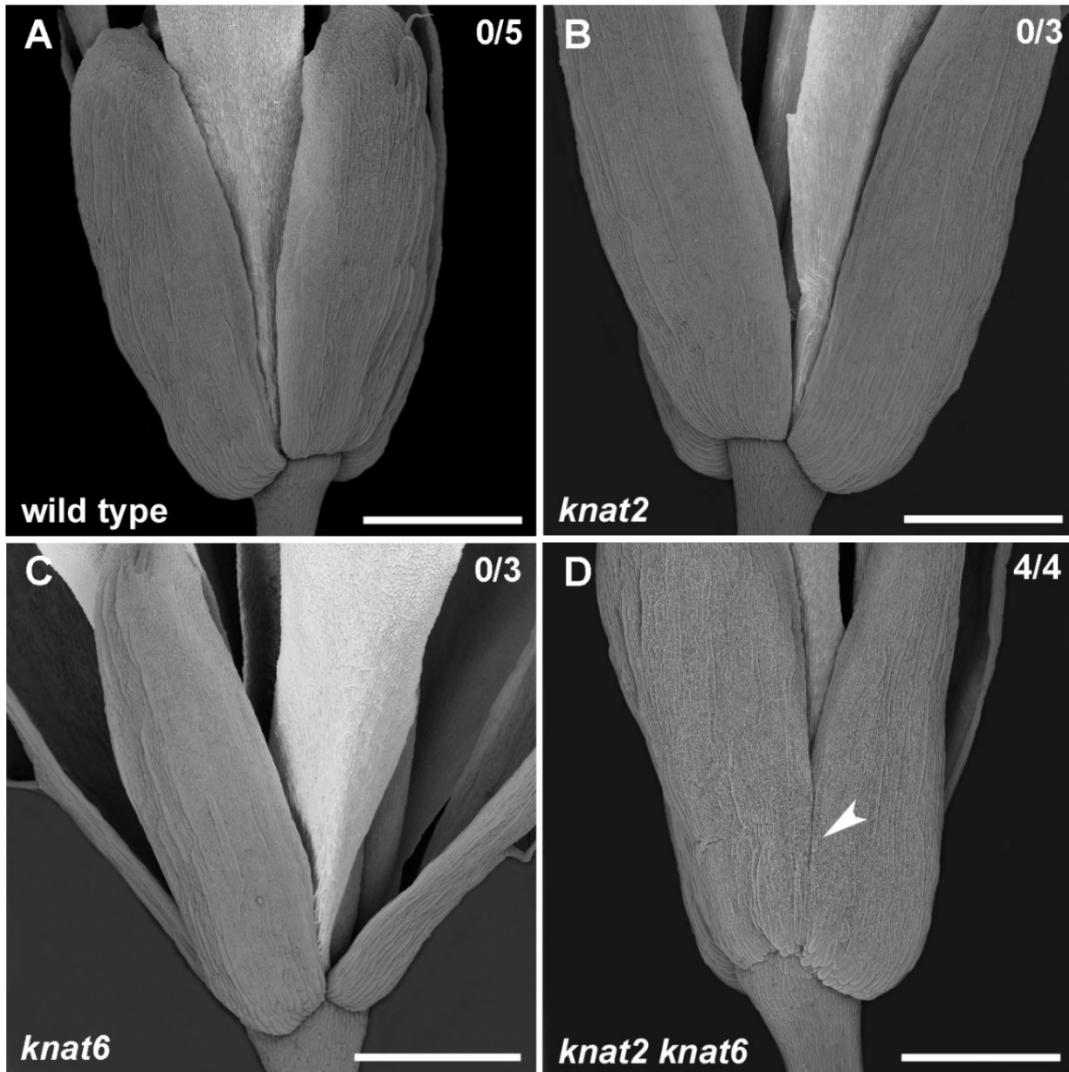
## SUPPLEMENTARY MATERIALS

**Supplemental Table S1. Abscission characteristic descriptions of mutant plants**

<b>Genotype</b>	<b>Abscission Position</b>	<b>Description</b>
wild type	6.4 ± 0.2	
<i>bop1 bop2</i>	N/A	No abscission. Floral organs at all positions rip when force is applied.
<i>BOP1 o/e</i>	4.9 ± 0.1	Premature abscission.
<i>bp-2</i>	5.7 ± 0.2	Premature abscission.
<i>ath1</i>	9.0 ± 0.2	Delayed abscission. Stamens remain lightly attached until far down the inflorescence.
<i>knat2</i>	6.6 ± 0.2	Similar to wild type.
<i>knat6</i>	7.1 ± 0.1	Similar to wild type.
<i>ath1 bp-2</i>	10.9 ± 0.8	Stamens remain lightly attached until far down the inflorescence. Similar to <i>ath1</i> .
<i>tga1 tga4</i>	6.1 ± 0.5	Similar to wild type.
<i>ath1 tga1</i>	7.8 ± 0.6	Delayed abscission. Stamens remain lightly attached until far down the inflorescence. Similar to <i>ath1</i> .
<i>ath1 tga4</i>	8.5 ± 0.2	Delayed abscission. Stamens remain lightly attached until far down the inflorescence. Similar to <i>ath1</i> .
<i>ath1 tga1 tga4</i>	8.1 ± 0.2	Delayed abscission. Stamens remain lightly attached until far down the inflorescence. Similar to <i>ath1</i> .
<i>ath1 knat2</i>	12.5 ± 0.7	Partial abscission in most cases, some petals are lightly attached far down the inflorescence but fall off with a tap. Stamens stay attached similar to <i>ath1</i> .
<i>ath1 knat6</i>	N/A	No abscission. Floral organs at late positions are cleanly removed when force is applied.
<i>knat2 knat6</i>	8.2 ± 0.1	Slight delay in abscission. Some floral organs remain loosely attached compared to wild type.
<i>ath1 knat2 knat6</i>	N/A	No abscission. Floral organs at late positions are cleanly removed when force is applied.

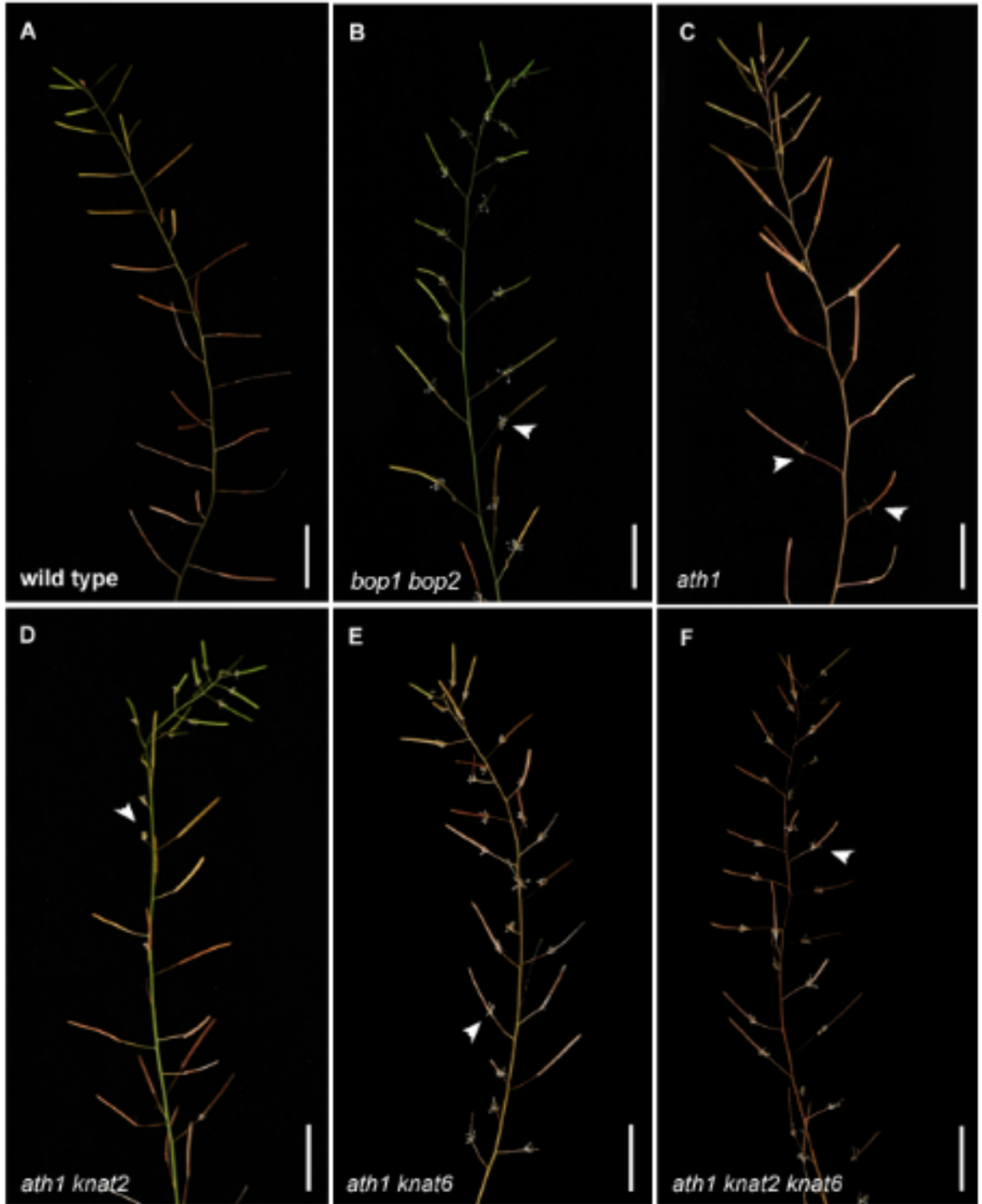
**Supplemental Table S2. List of qPCR primers**

Gene	Primers	Sequence (5' to 3')	Source
IDA	IDA-FWD-06/18	CAATGGCTCCGTGTCGT	Chris
	IDA-REV-06/18	TCAATGAGGAAGAGAGTTAACAAAAGAG	Bergin
HAE	HAE-FWD-06/18	CGCGATGTGAAGTCGAGTAA	Chris
	HAE-REV-06/18	GTGTATACGTATTCTGGTGCAATG	Bergin
NEV	NEV-FWD-06/18-1	AAAGCCAACGTCTCTAAGGAG	Chris
	NEV-REV-06/18-1	ACACTAGCCCATCTTGGACCT	Bergin



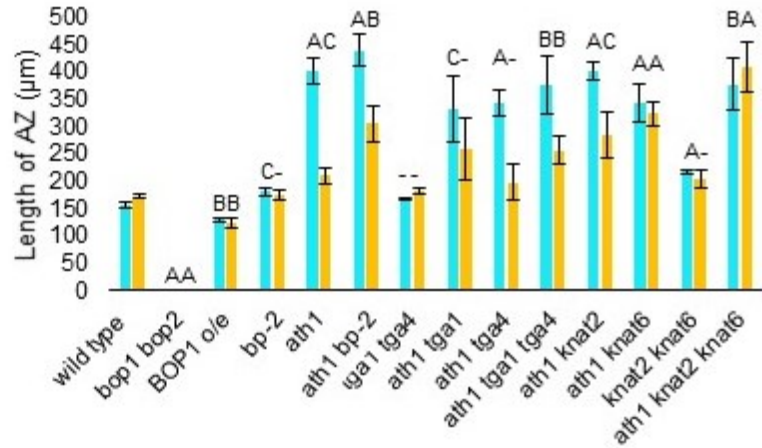
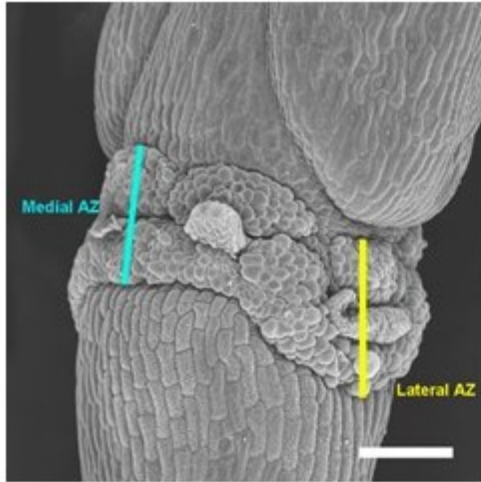
**Supplemental Figure S1. SEM images of wild type and boundary gene mutants.**

Representative images showing position 2 flowers. Numbers at the top right of panels indicate frequency of sepal-fusion defects. A, wild type showing well-separated sepals. B-C, *knat2* and *knat6* mutant showing no fusion of the sepals. D, *knat2 knat6* showing frequent strong fusion of sepals and smooth boundaries at the base of the flower (arrow heads). Scale bars: 500  $\mu$ m.



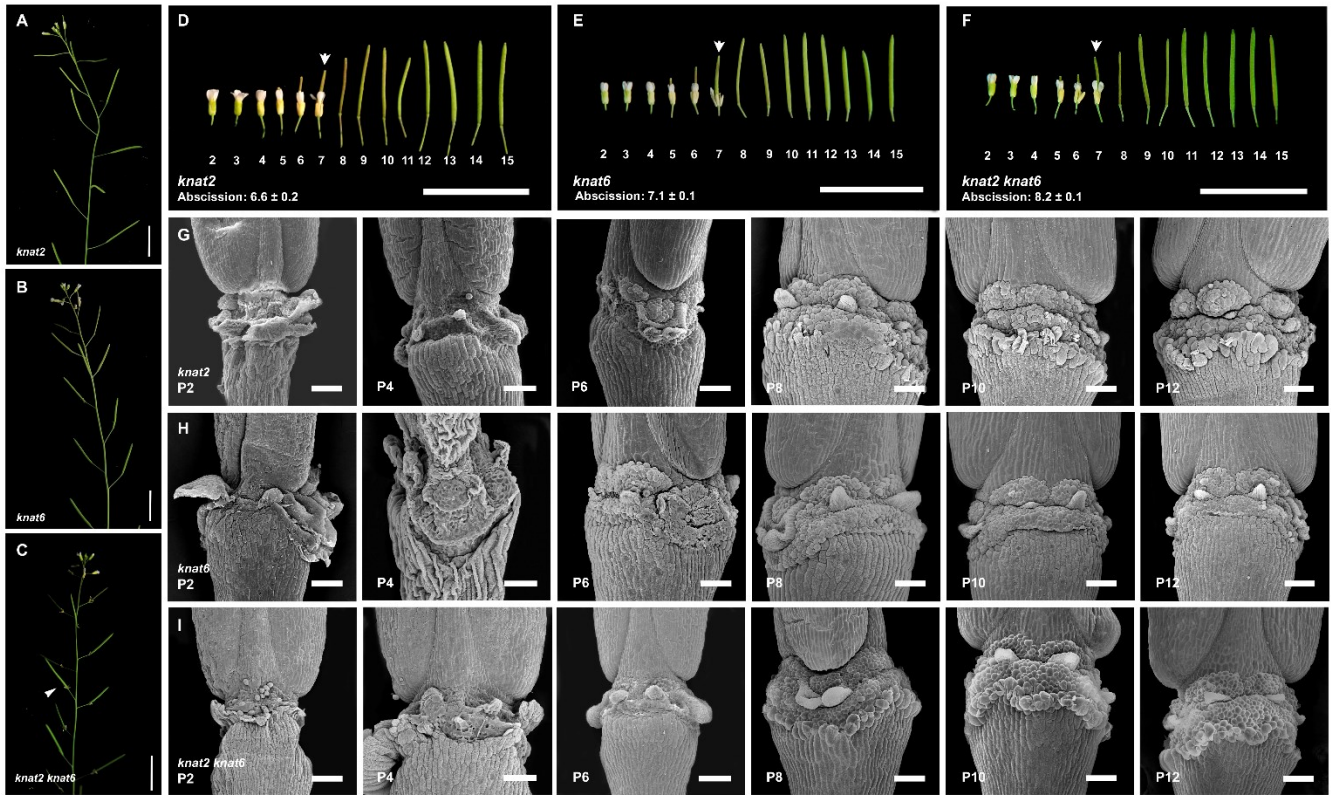
**Supplemental Figure S2. Inflorescence apices showing the abscission phenotype of 12-week-old wild type and mutant plants.**

Plants were grown under long-days. A, wild type showing complete abscission. B, *bop1 bop2* mutant, organs remain attached (arrow head). C, *ath1* mutant showing near-complete abscission (arrow heads, a few stamens remain loosely attached). D, *ath1 knat2* mutant, similar to *ath1* (arrow head, a few stamens remain loosely attached). E, *ath1 knat6* mutant, organs remain attached (arrow head). F, *ath1 knat2 knat6* mutant, organs remain attached (arrow head). Scale bars: 1.5 cm.



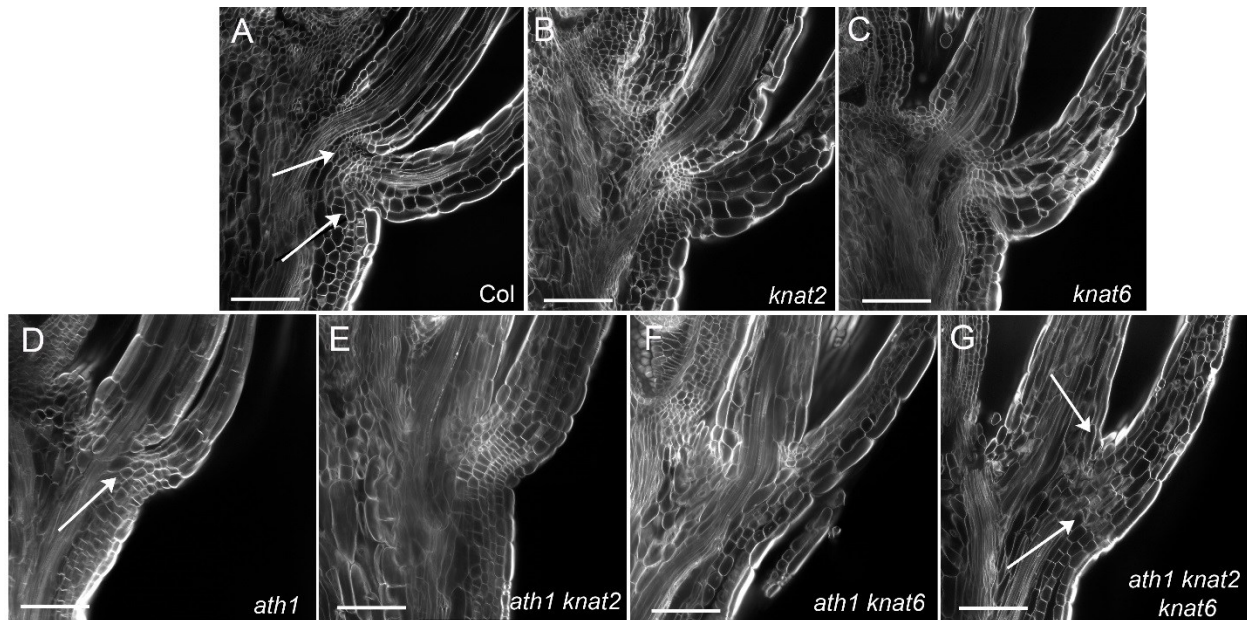
**Supplemental Figure S3. Measurement of medial and lateral AZ in wild type and mutants.**

(Left) SEM image of position 12 wild type receptacle with labeled medial and lateral AZ. Scale bar: 100 µm. (Right) Graph showing the average length of medial and lateral AZs of wild type and mutants at position 12 based on SEM images (n=5 fruits per node per genotype). Error bars, standard error. Letters represent significant differences compared to wild type (student t-test): A, extremely statistically significant; B, very statistically significant; C, statistically significant; - not statistically significant.



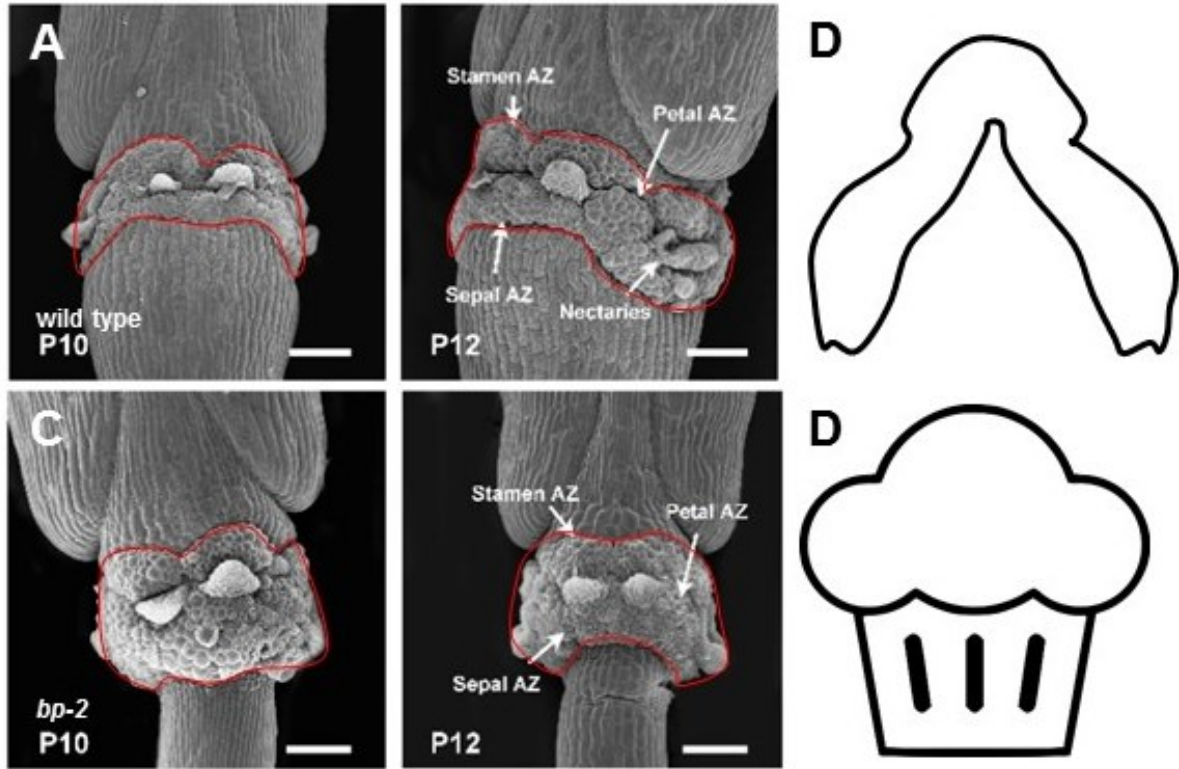
**Supplemental Figure S4. Abscission analysis of *knat2*, *knat6* and *knat2 knat6* mutants.**

Representative images are shown. A-C, Inflorescence apices. *knat2* and *knat6* shed their floral organs similar to wild type while *knat2 knat6* partially retain their floral organs. Arrow head, floral organs that are retained by mutants with abscission defect. D-F, Abscission series of mutant flowers/fruits at positions 2-15 on the inflorescence. Arrow heads, initiation of abscission defined as the position at which organs start to detach with gentle mechanical touch. Numerical data (bottom left) indicate mean position for initiation of abscission ± standard error (n=20 plants per genotype). F, *knat2 knat6* showing a slight delay in abscission compared to wild type. G-I, SEM micrographs showing mutant AZs at positions 2, 4, 6, 8, 10, and 12 on the inflorescence. G, *knat2* showing slight enlargement of sepal AZ cells compared to wild type. H, *knat6* showing similar to wild type. I, *knat2 knat6* showing slightly enlarged AZs compared to wild type. For wild type, see Figure 3.4A. Scale bars: A-F, 1.5 cm; G-I, 100 μm.



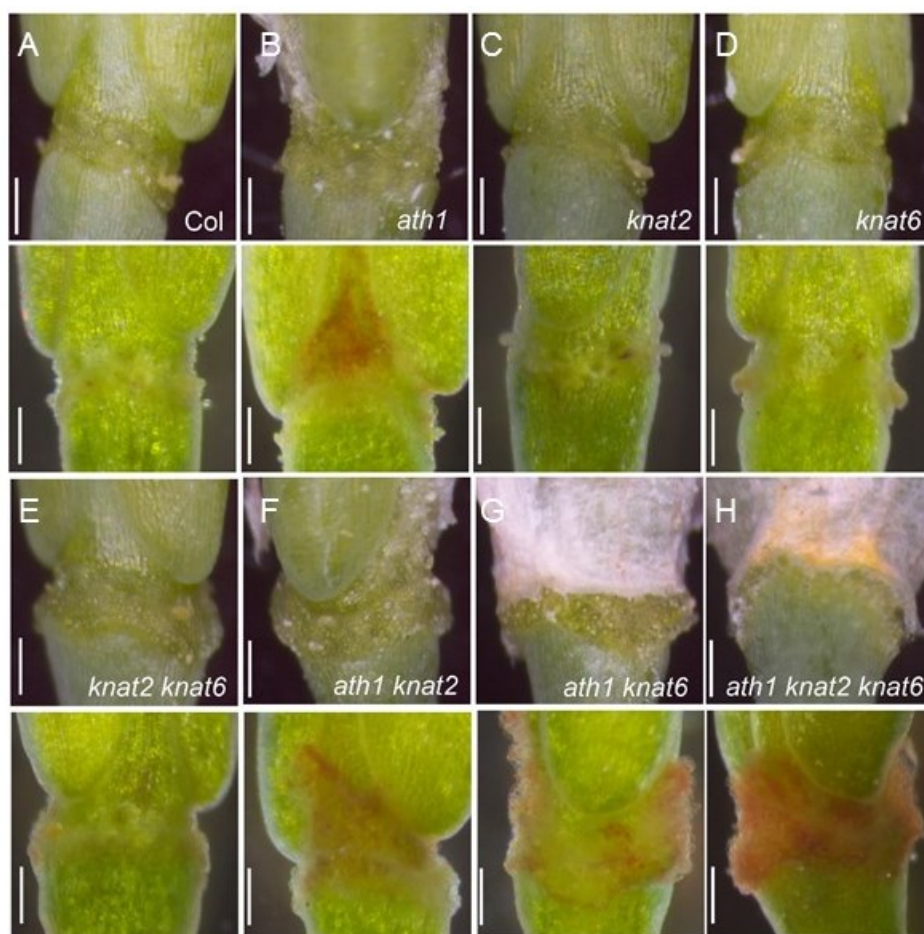
**Supplemental Figure S5. Morphology of floral AZs in wild type and mutants.**

Representative confocal cross-sections of mature flowers are shown. A, wild type showing distinct small AZ cells at the stamen filament-receptacle junction (arrows). B-C, *knat2* and *knat6* mutants showing stamen filament-receptacle junctions similar to wild type. D, *ath1* mutant showing lack of distinct AZ cells and a reduced constriction at the base of the stamen filament (arrow). E, *ath1 knat2* mutant showing indistinct AZ cells similar to *ath1*. F, *ath1 knat6* mutant showing further impairment of AZ cells compared to *ath1* and little or no constriction at the base of the stamen filament. G, *ath1 knat2 knat6* mutant showing lack of AZ morphology and no constriction at the base of the stamen filament. Figure by Véronique Pautot. Scale bars: 1 mm.



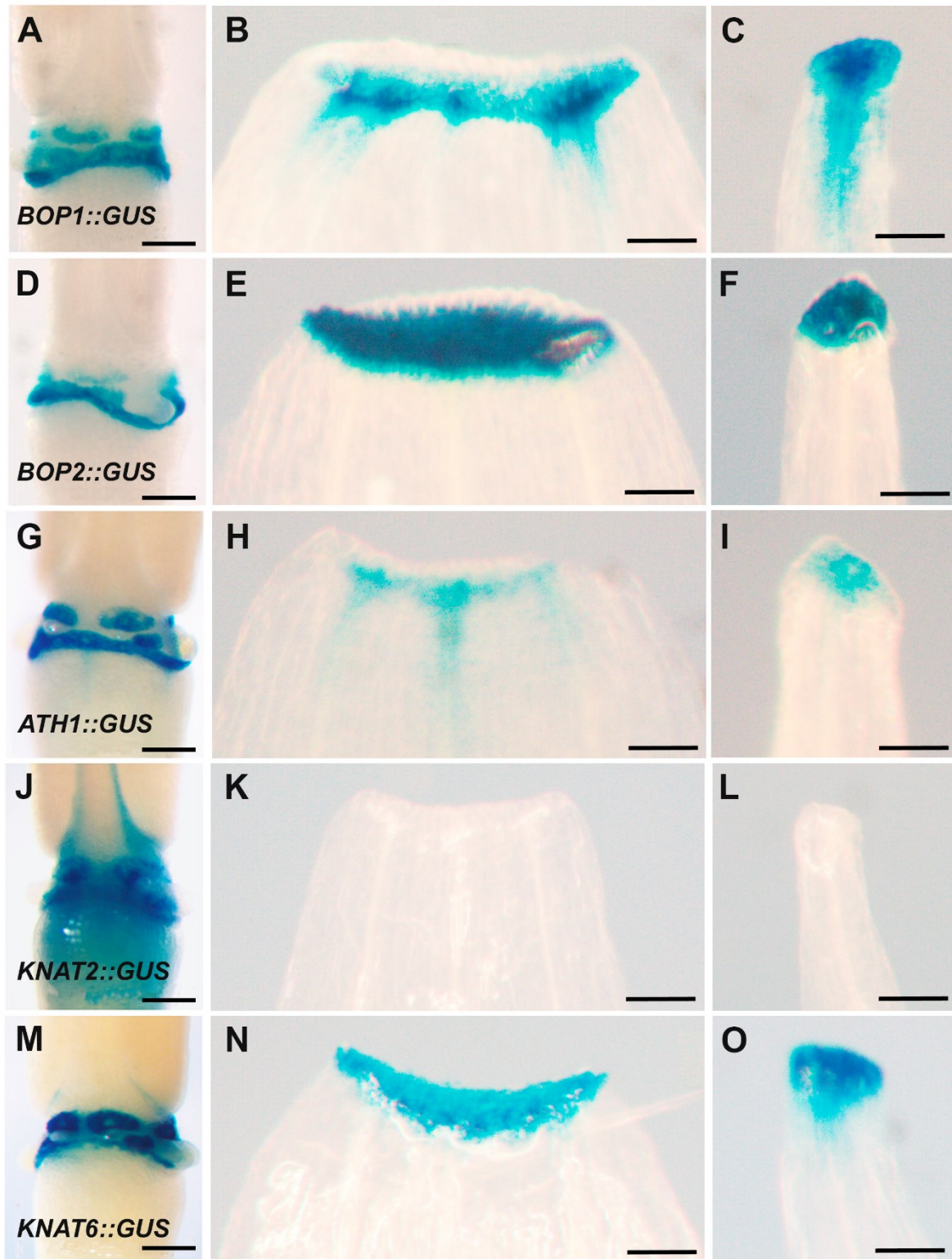
**Supplemental Figure S6. Comparing AZ shape of wild type and *bp-2* mutant.**

Images show position 10 and 12 flowers. A, wild type receptacles with red border exaggerating the “saddle” AZ shape. B, a front view of a horse saddle for comparison to wild type AZ. C, *bp-2* receptacles with red border exaggerating the “muffin top” AZ shape. D, a drawing of a muffin for comparison to *bp-2* AZ. Scale bars: 100  $\mu\text{m}$ .



**Supplemental Figure S7. Wild-type and mutant siliques stained with Yariv reagent for detection of arabinogalactans in the AZ.**

$\beta$ -D-glucosyl Yariv ( $\beta$ -glcY) reagent is a diagnostic stain for arabinogalactans, indicated by a red precipitate (Stenvik et al., 2006). Plants overexpressing IDA accumulate this substance in AZs (Stenvik et al., 2006). Floral organs at the base of wild-type and mutant fruits were allowed to abscise naturally or dissected to expose the AZ. A-H, Top row shows siliques before staining and bottom row shows siliques after staining. Arabinogalactans overaccumulate in *ath1*-containing single, double, and triple mutants. Figure by Véronique Pautot. Scale bars: 20  $\mu$ m.



**Supplemental Figure S8. Promoter GUS fusions showing the expression of boundary genes in residuum and secession AZ layers.**

Siliques (A, D, G, J, M) and detached sepals (B, E, H, K, N) and petals (C, F, I, L, O) were stained for GUS activity at position 5-6 (just after abscission). Figure by Véronique Pautot. Reporters are described in (Dockx et al., 1995; Belles-Boix et al., 2006; Khan et al., 2015). Scale bars: 1 mm except A, D, G, J, M: 100  $\mu$ M.